POLITECNICO
MILANO 1863

SCUOLA DI INGEGNERIA INDUSTRIALE
E DELL'INFORMAZIONE

Simulation and control of a thermo-hydraulic system

TESI DI LAUREA MAGISTRALE IN
AUTOMATION AND CONTROL ENGINEERING
INGEGNERIA DELL'AUTOMAZIONE

Author: **Aydin Nasirzade**

Student ID: 943555
Advisor: Prof. Riccardo SCATTOLINI
Academic Year: 2021-22

Acknowledgments

I dedicate this paper to my late brother who tragically left this world last year. I will forever be grateful for his existence in my life. My heart indescribably aches that he could not live enough to see me graduate. But I know that he would have been proud of me. His memories will always continue to feel me loved.

I would like to show my deepest gratitude to Prof. Riccardo Scattolini, my thesis supervisor, for his patience, inspiration, and guidance during the development of this work. His willingness to allot time to me is truly appreciated, even though I have never deserved the privilege to work with him. I thank him for not giving up on me during the most trying and miserable times of my life. I will always keep this gratitude to him for being the only light in the darkest phase of my academic career.

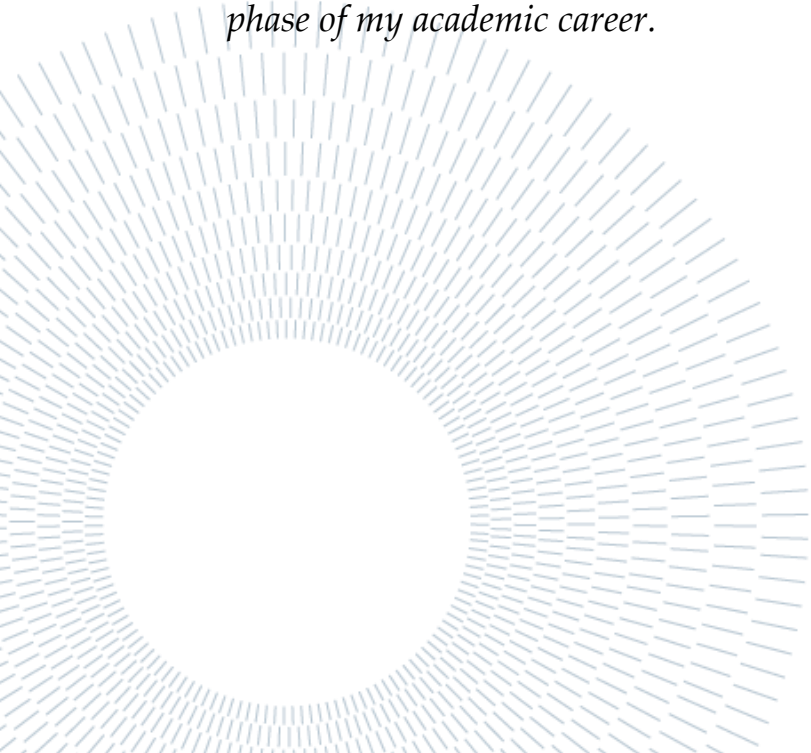

Abstract

The focus of this thesis is to model, simulate and control a nonlinear thermo-hydraulic plant by different control strategies. The aim of the control is to achieve a zero steady-state error in the controlled variable, the water temperature, which is one of the two states of the thermo-hydraulic system. The work is carried out after studying the system's different operating conditions, and various stability characteristics. Additionally, we obtain a linearized model with which the main characteristics of the system are examined. The simulator of the system is designed based on these analyses in the MATLAB/Simulink, after which numerous control techniques are used to reject external disturbances on the system. We start this by a classical PI controller, which later is followed by a pole-placement technique where one relocates the poles of the system to obtain a desired response. Moreover, LQ and LQG design techniques are also considered in this paper. These methods require converting the control design problems into an optimization problem with some performance criteria in time-domain. In the LQG control stochastic processes are used to model measurement noises and disturbances. However, in most applications it is challenging to model exact stochastic properties of noises and disturbances. Therefore, we have considered another technique in which the stochastic elements of the LQG control are removed. This control method is called the H_2 control of which the LQG control can be seen as a specific case. In this thesis, another class of controllers harnessed is the H_∞ control, which is followed by backstepping. The latter is a control method in which a control law developed guarantees asymptotic stability based on the Lyapunov theorem. Throughout the thesis, necessary figures, equations, tables are reported too. The simulation results show that the controllers synthesized provide a satisfactory setpoint tracking. Finally, a comparative analysis is given at the end to decide which controller works best for disturbance rejection and zero-error tracking of the thermo-hydraulic system response.

Key words: thermo-hydraulic plant, PI control, pole placement, Linear Quadratic (LQ) control, Linear Quadratic Gaussian (LQG) control, Kalman filters, H_2 control, H_∞ control, backstepping

Abstract in italiano

L'obiettivo di questa tesi è modellare, simulare e controllare un impianto termoidraulico non lineare mediante diverse strategie di controllo. Lo scopo del controllo è di ottenere un errore stazionario nullo nella variabile controllata, la temperatura dell'acqua, che è uno dei due stati del sistema termo-idraulico. Il lavoro viene eseguito dopo aver studiato le diverse condizioni operative del sistema e le diverse caratteristiche di stabilità. Inoltre, otteniamo un modello linearizzato con il quale vengono esaminate le principali caratteristiche del sistema. Il simulatore del sistema è progettato sulla base di queste analisi in MATLAB/Simulink, dopodiché vengono utilizzate numerose tecniche di controllo per reiettare i disturbi esterni al sistema. Iniziamo con un controller PI classico, che è seguito da una tecnica di posizionamento dei poli in cui si riposizionano i poli del sistema per ottenere la risposta desiderata. Inoltre, in questo documento vengono considerate anche le tecniche di progettazione LQ e LQG. Questi metodi richiedono la conversione del problema di progettazione del controllo in un problema di ottimizzazione con alcuni criteri di prestazione nel dominio del tempo. Nel controllo LQG vengono utilizzati i processi stocastici per modellare rumori e disturbi di misurazione. Tuttavia, nella maggior parte delle applicazioni è difficile modellare esatte proprietà stocastiche di rumori e disturbi. Pertanto, abbiamo considerato un'altra tecnica in cui vengono rimossi gli elementi stocastici del controllo LQG. Questo metodo di controllo è chiamato controllo H_2 di cui il controllo LQG è un caso specifico. In questa tesi, un'altra classe di controllori considerati è il controllo H_∞, seguito da backstepping. Quest'ultimo è un metodo di controllo in cui la legge di controllo sviluppata garantisce stabilità asintotica basata sul teorema di Lyapunov. In tutta la tesi sono riportate anche le figure necessarie, le equazioni, le tabelle. I risultati della simulazione mostrano che i controllori sintetizzati forniscono un tracking del setpoint soddisfacente. Infine, viene fornita un'analisi comparativa al fine di decidere quale controllore funziona meglio per la reiezione dei disturbi e il monitoraggio a zero errori della risposta del sistema termo-idraulico.

Contents

List of Figures

List of Tables

Introduction

Nowadays one of the most commonly used systems for heat exchange is a thermo-hydraulic plant. In this thesis, analytical modelling, simulation and various control means of this system are investigated.

In Chapter 1, the system description is given. The chapter covers the physical properties of a thermo-hydraulic plant. The thermo-hydraulic system is a two-state non-linear system with 3 inputs and 2 outputs. The most common fluid that is used in the thermo-hydraulic systems is water since it is the safest, less poisonous and cheaper material for heat transfer. In the thermo-hydraulic plants, water enters the system with a flow rate w at a particular temperature T_i, resulting in a constant level z. In the chamber of the plant the temperature of the water T is manipulated by the gas flow rate w_c through a control valve. Thus, the flame of the temperature T_f changes the temperature of the metal at the base of the chamber. The heated water exits the chamber at the same flowrate w and the temperature T. After introducing the mathematical equation of the system in Chapter 1, it is linearized around 5 different operating points. At the end of the chapter, some parameters, such as eigenvalues, static gains, open-loop step responses of the linearized system are studied.

After linearization around the central operating point ($\overline{w} = 1$), the open-loop transfer function matrix is derived, from which the transfer function from w_c (control variable) to T (system output) is chosen specifically for disturbance (caused by the load flow rate w) rejection in the thermo-hydraulic system with different control strategies in Chapter 2. We start by using the classical control strategy, a PI controller, which is followed by a state-feedback law, i.e., a pole-placement control technique. Note that after introducing the theoretical development of the pole-placement control, we implement this strategy to a SISO system to control the whole non-linear plant. However, later the system is augmented with an integrator through the control loop from w_c to T, on which the pole-placement is implemented. Next, some optimal control techniques are used, such as the LQ control. This is a control technique in which we use mathematical equations to reduce a cost function with specified weighting factors. The LQ control is partly a solution to the next control method, LQG, we consider in Chapter 2. The LQG control, being another fundamental optimal control problem, is seen as a combination of the Kalman

filtering and the LQ control. Later in the chapter, two more controllers are designed for disturbance rejection, namely H_2 and H_∞ controllers, in which shaping functions are used to get the desired frequency-domain characteristics. At the end of the chapter, the backstepping control strategy is developed.

In Chapter 3, we study the differences of the controllers synthesized based on their setpoint tracking and control actions. At last, conclusions are drawn, and some possible future developments are put forward in the final chapter. Note that Appendix A is reported at the end of the thesis to enrich its content.

1 The thermo-hydraulic system

In this chapter, the physical properties of a thermo-hydraulic plant are given together with its non-linear mathematical equations. Later the system is linearized around 5 different operating points, and the characteristics of the linearized models are compared.

1.1. System description

The schematic diagram of a thermo-hydraulic plant is given below.

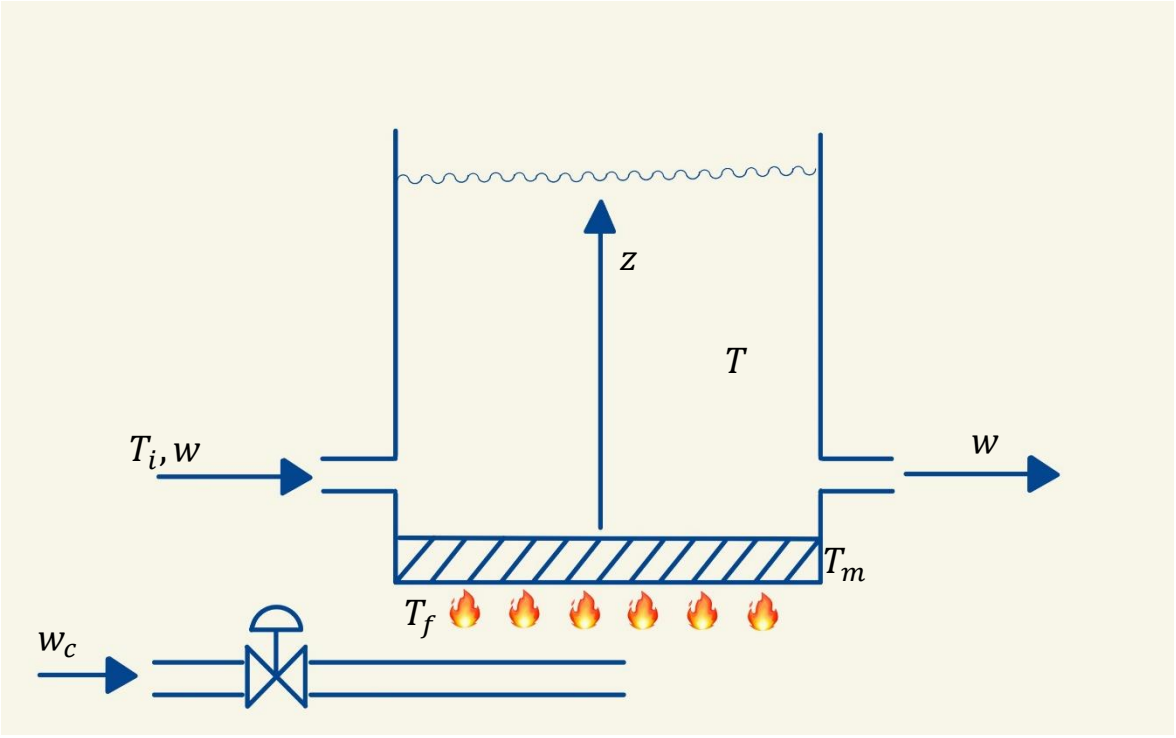

Figure 1.1: Thermo-hydraulic system

The variables shown in Figure 1.1:

- w - load flow rate

- T- temperature of water (controlled variable)
- T_i - inlet load temperature
- w_c - gas flowrate: control variable
- z - (constant) level
- T_f- temperature of the flame
- T_m- temperature of the metal

The control goal is to design and test different control structures that aim to sustain the variable T at the desired reference value rejecting the disturbances w. This system's dynamics are non-linear and characterized by the following 2 state-space equations:

$$\begin{cases} \dfrac{dT}{dt} = \dfrac{1}{\rho A z}\left[w(T_i - T) + \dfrac{k_{lm}A}{c}(T_m - T)\right] \\ \dfrac{dT_m}{dt} = \dfrac{1}{M_m c_m}\left[-k_{lm}A(T_m - T) + \sigma k_f w_c (T_f^4 - T_m^4)\right] \end{cases}$$

where:

Variable	Values	Units	Description
$\boldsymbol{A}$	$\frac{\pi}{4}$	m^2	Area of the section of the tank
ρ	900	$\frac{kg}{m^3}$	Water density
$\boldsymbol{c}$	4180	$\frac{J}{kgK}$	Specific heat of the water
$\boldsymbol{M_m}$	617.32	kg	Mass of the metal
$\boldsymbol{c_m}$	418	$\frac{J}{kgK}$	Specific heat of the metal
$\boldsymbol{k_{lm}}$	3326.4	$\frac{kg}{s^3K}$	Heat exchange coefficient
$\boldsymbol{\sigma}$	$5.67 \cdot 10^{-8}$	$\frac{W}{m^2K^4}$	Radiation coefficient
$\boldsymbol{T_f}$	1200	K	Temperature of the flame
$\boldsymbol{k_f}$	8	$\frac{m^2 s}{kg}$	Valve coefficient

Table 1.1: Physical parameters of the system

It is obvious from Figure 1.1 that the inputs of the system are load flow rate (w), gas flowrate (w_c), temperature of the flame (T_f, assumed to be always constant) and inlet load temperature (T_i), whereas the states are the temperature of the water (T) and the temperature of the metal (T_m).

The thermo-hydraulic plant's dynamics and behavior are analyzed with a software package (Simulink), as shown in Figure 1.2.

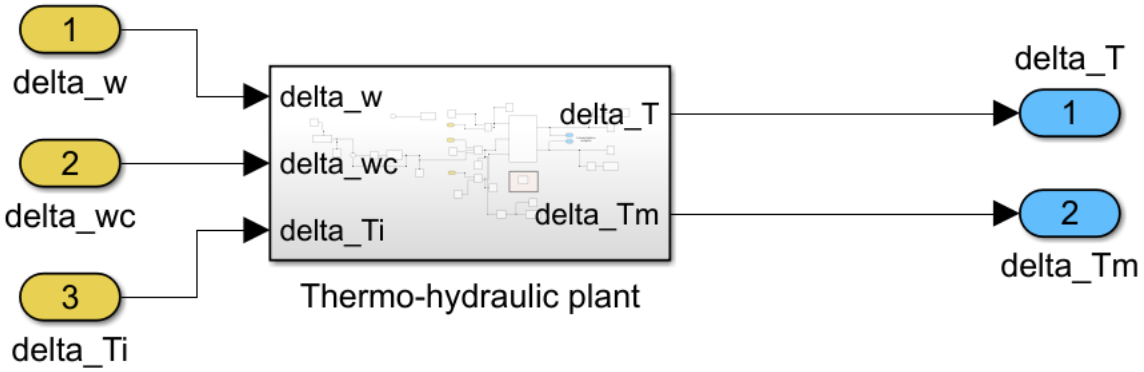

Figure 1.2: Thermo-hydraulic plant with its inputs and outputs

For more detailed information on the Simulink blocks and script codes, you can refer to Appendix A.

1.2. Linearization

In this chapter, a few equilibrium points are defined, after which we are going to linearize the nonlinear thermo-hydraulic system around these points. The necessary procedure for one equilibrium point has been given explicitly to avoid repetitiveness in Section 1.3, where the linearization takes place for four other equilibrium conditions.

The nonlinear system is linearized so that we can understand its properties and characteristics in a corresponding operating point. This is done for a few reasons to mention, such as we can check the local stability of the system and the system dynamics easily, how a non-linear system behaves (at least in the neighborhood of equilibrium points), we can speed up simulations of the original system having the linearized version of it. Moreover, we have many tools (e.g., Simulink) for non-linear control design that can produce linearized models and their transfer functions, state-space, pole-zero-gain equations, which in turn can be used to plot Bode diagrams, to analyze system response in different operating points, to design a linear controller, etc.

Below is given a table that demonstrates some equilibria (*e1*, *e2*, *e3*, *e4*, *e5*) corresponding to different loads (*w*).

	e1	e2	e3	e4	e5
$\bar{w}$	0.5	0.75	1	1.25	1.5
$\bar{T}_i$	298	298	298	298	298
$\bar{T}$	323	323	323	323	323
$\bar{T}_m$	343	353	363	373	383
$\bar{w}_c$	0.0559	0.084	0.112	0.1402	0.1684

Table 1.2: Some equilibria corresponding to different loads

For the given system $\dot{x}(t) = f(x(t), u(t))$ assuming that $f(x, u)$ is continuously differentiable with respect to its arguments and setting

$$x(t) = \bar{x} + \delta x(t)$$

$$u(t) = \bar{u} + \delta u(t)$$

the linearized system takes the following form:

$$\delta\dot{x}(t) = A\delta x(t) + B\delta u(t)$$

where

$$A = \left.\frac{\partial f}{\partial x}\right|_{x=\bar{x},u=\bar{u}}$$

$$B = \left.\frac{\partial f}{\partial u}\right|_{x=\bar{x},u=\bar{u}}$$

In this thesis numerical linearization is computed by means of Simulink. Before going into linearization, let's consider equilibrium point, as an example, for $\bar{w} = 1$. To find out equilibrium, we need to set the original differential system equation to zero.

$$\dot{T}(t) = 0;\ \dot{T}_m(t) = 0$$

We set, T to $\bar{T}$, T_m to $\bar{T}_m$, T to $\bar{T}_i$, w to $\bar{w}$, w_c to $\bar{w}_c$ and suitably substitute in the above-given equations.

$$\begin{cases} 0 = \dfrac{1}{\rho A z}\left[\bar{w}(\bar{T}_i - \bar{T}) + \dfrac{k_{lm}A}{c}(\bar{T}_m - \bar{T})\right] \\ 0 = \dfrac{1}{M_m c_m}\left[-k_{lm}A(\bar{T}_m - \bar{T}) + \sigma k_f \bar{w}_c(\bar{T}_f^4 - \bar{T}_m^4)\right] \end{cases}$$

After analytically solving these equations, we get the equilibrium point corresponding to $w = 1$, given the target temperature of the water equal to 323. As mentioned earlier, there are three unknown inputs, and their equilibrium values are as follows.

$$\bar{w} = 1.0000$$

$$\bar{w}_c = 0.1120$$

$$\bar{T}_i = 298$$

Note that, from the first equation, if you fix $\bar{w}, \bar{T}_i$ and $\bar{T}$, then $\bar{T}_m$ is automatically fixed. This is the way to compute equilibria. In the same way, once $\bar{T}, \bar{T}_m, \bar{w}$ are fixed, and being $\bar{T}_f$ fixed, from the second equation you immediately compute $\bar{w}_c$.

For the equilibrium point, we can also analyze the phase-plane, i.e., the state trajectories reported in Figures 1.3 and 1.4. By doing that we can study system behavior for a given initial condition. We use the MATLAB script (*pplane*) to realize it:

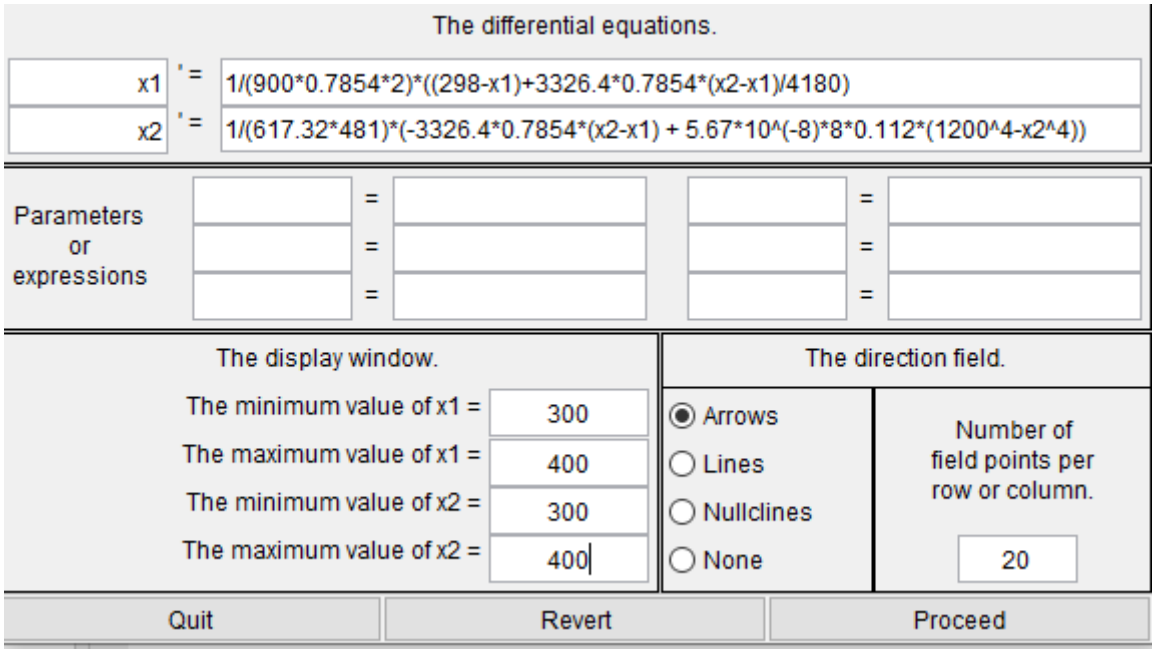

Figure 1.3: Phase plane GUI

After proceeding, we get the following sketch:

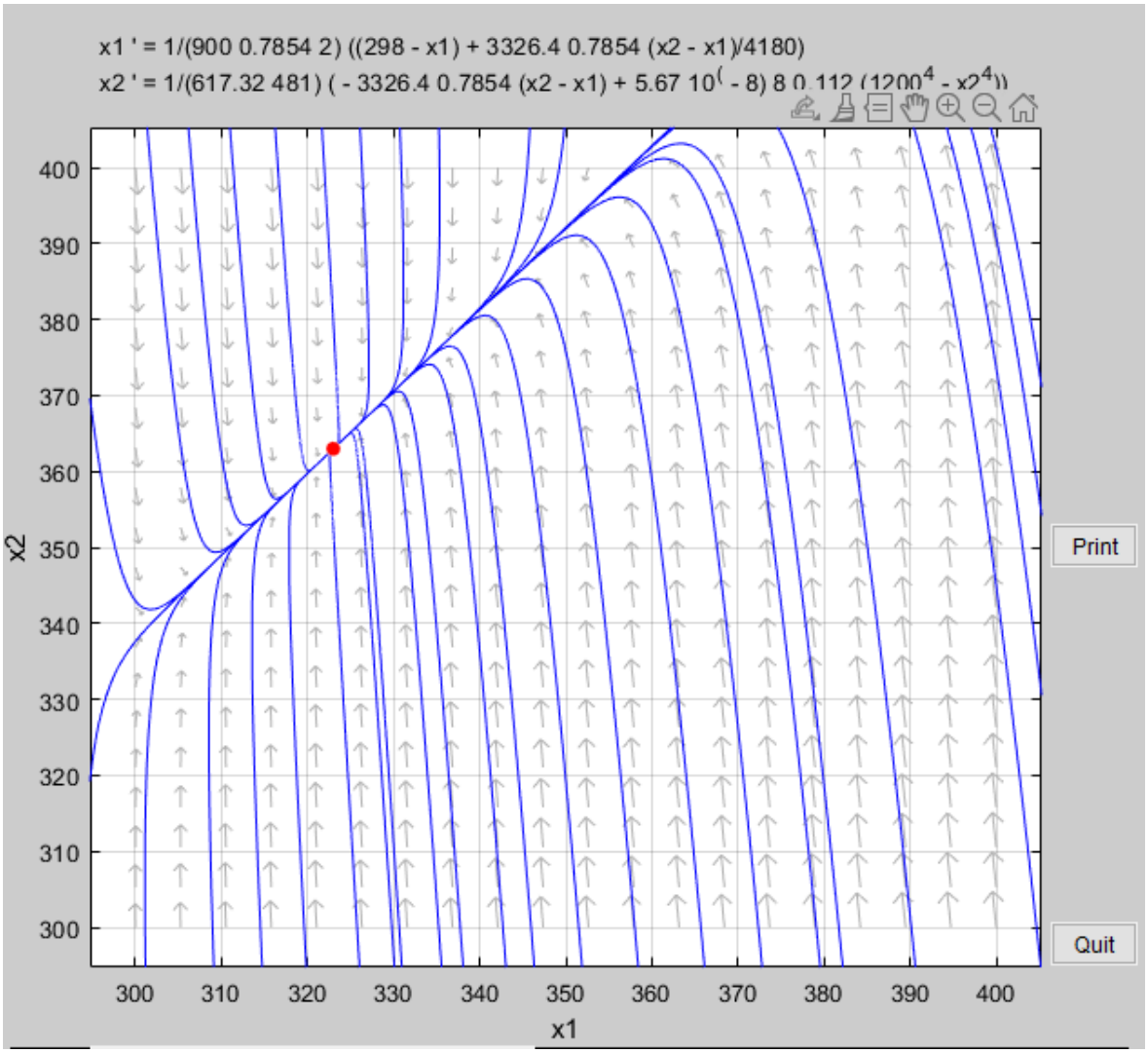

Figure 1.4: State trajectories

As can be seen from Figure 1.4, the phase plane shows that the equilibrium is a stable node. The eigenvalues of the linearized system are reported in the following table:

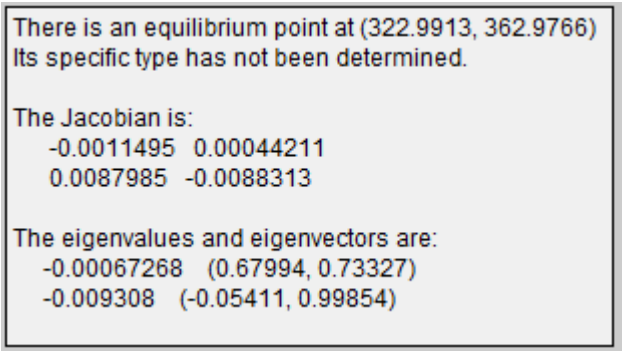

Figure 1.5: Phase plane results on Jacobian and eigenvalues

Now let's find out the linearized system around the first choice of equilibrium points shown above. For this to occur, we decided to use *Time-Based Linearization* block in Simulink. This block calls basic linearization functions to generate a linear model for a given system. The linearization happens when the time determined (T=10000 in our case) is reached by the simulation clock and where the system is for sure at an equilibrium. The linearized model later is stored as a structure in Workspace in MATLAB. The structure contains some useful information, such as A, B, C, D matrices of the linear model, names of model's states and outputs, and so forth.

After specifying inputs and outputs of the perspective linear system's transfer function (that Time-Based Linearization block will track), we add equilibrium points of the inputs. After running the simulation, it turns out that the linearized system's state space matrices corresponding to the considered equilibrium are as follows:

$$A = \begin{bmatrix} -0.0011 & 0.0004 \\ 0.0088 & -0.0088 \end{bmatrix} \qquad B = \begin{bmatrix} -0.0167 & 0 & 0.0007 \\ 0 & 3.1422 & 0 \end{bmatrix}$$

$$C = \begin{bmatrix} 1 & 0 \\ 0 & 1 \end{bmatrix} \qquad D = \begin{bmatrix} 0 & 0 & 0 \\ 0 & 0 & 0 \end{bmatrix}$$

From matrix A, it can be computed that the eigenvalues, thus the poles of the linearized system are: -0.0007 and -0.0093, both being stable. It is worth mentioning that the phase plane in Figure 1.5 shows almost the same results for both eigenvalues and Jacobians.

To derive a transfer function of any linearized system from its state-space representation, we need to use a conversion method. Considering a MIMO system given below:

$$\dot{x}(t) = Ax(t) + Bu(t)$$

$$y(t) = Cx(t) + Du(t)$$

with $x \epsilon R^n, u \epsilon R^m, y \epsilon R^p$, the corresponding matrix of transfer functions is computed as:

$$G(s) = C(sI - A)^{-1}B + D = \begin{bmatrix} G_{11}(s) & \cdots & G_{1m}(s) \\ \vdots & \ddots & \vdots \\ G_{p1}(s) & \cdots & G_{pm}(s) \end{bmatrix}$$

where in the Laplace domain, the following relationship holds:

$$Y(s) = G(s)U(s)$$

The equation of $G(s)$ is used to transform a given state-space representation to a transfer function form. Therefore, the open-loop transfer function of our linearized system becomes 2x3 matrix $G_{ol}(s)$, with 3 inputs and 2 outputs (MATLAB code in Appendix A):

$$G_{ol}(s) = \begin{bmatrix} \frac{-0.01674s - 0.0001478}{s^2 + 0.009978s + 6.258 \cdot 10^{-6}} & \frac{0.001389}{s^2 + 0.009978s + 6.258 \cdot 10^{-6}} & \frac{0.0007074\, s + 6.245 \cdot 10^{-6}}{s^2 + 0.009978s + 6.258 \cdot 10^{-6}} \\ \frac{-2.219 \cdot 10^{-17}\, s - 0.0001472}{s^2 + 0.009978s + 6.258 \cdot 10^{-6}} & \frac{3.142\, s + 0.003612}{s^2 + 0.009978s + 6.258 \cdot 10^{-6}} & \frac{9.38 \cdot 10^{-19} s + 6.224 \cdot 10^{-6}}{s^2 + 0.009978s + 6.258 \cdot 10^{-6}} \end{bmatrix}$$

This matrix of transfer functions outlines the separate transfer functions from inputs of the thermo-hydraulic system to its outputs. Let's take $G_{ol_{1,1}}(s)$ as an example. It is a transfer function from the first input (w) to the first output (T). Likewise, the following transfer functions correspond to their associated input-output pairs:

$G_{ol_{1,2}}(s)$ – an open-loop transfer function from w to T_m

$G_{ol_{2,1}}(s)$ – an open-loop transfer function from w_c to T

$G_{ol_{2,2}}(s)$ – an open-loop transfer function from w_c to T_m

$G_{ol_{3,1}}(s)$ – an open-loop transfer function from T_i to T

$G_{ol_{3,2}}(s)$ – an open-loop transfer function from T_i to T_m

1.3. Comparative analysis of different equilibrium conditions

In this section, we linearize the thermo-hydraulic system around four more equilibria, thus a table of the eigenvalues at the different operating points are provided. Furthermore, we are going to consider static gains from w_c to T and step responses of the 5 operating points along with their Bode diagrams.

1.3.1. Eigenvalues of the linearized system

To find poles of a MIMO system, one needs to know that in a minimal form, the poles of the system coincide with eigenvalues of the state matrix A, or in other words, with the roots of the characteristic equation:

$$\phi(s) = \det(sI - A) = 0$$

We compute the poles of a MIMO system directly from the transfer function, i.e., $\phi(s)$, which is the characteristic polynomial corresponding to a minimal realization of the system which is represented by a transfer function $G(s)$ and is the least common denominator of all the non-null minors of $G(s)$.

After linearization of the system around five different operating points, we end up with the following eigenvalues in Table 1.3.

Operating points	**Eigenvalues**	
e1	-0.0003	-0.0093
e2	-0.0005	-0.0093
e3	-0.0007	-0.0093
e4	-0.0008	-0.0093
e5	-0.0010	-0.0093

Table 1.3: Eigenvalues corresponding to 5 operating points

It is interesting to note that the linearized system is faster and faster as the input $\overline{w}$ becomes larger and larger.

1.3.2. Static gains

In this paragraph, we consider the static gain from w_c to T. Since for linear asymptotically stable systems, the term "gain" can be differently used, it is better to specify the following notations. Generally, for a given frequency of ω the gain is defined as:

$$\frac{\|Y(j\omega)\|_2}{\|U(j\omega)\|_2} = \frac{\|G(j\omega)U(j\omega)\|_2}{\|U(j\omega)\|_2}$$

assuming that $Y(s) = G(s)U(s)$ and that the Fourier transfer of the input is $U(j\omega)$. It turns out that the gain for a SISO system at a given frequency ω is $|G(j\omega)|$. However, consider the following relation for MIMO systems:

$$\underline{\sigma}(G(j\omega)) \leq \frac{\|G(j\omega)U(j\omega)\|_2}{\|U(j\omega)\|_2} \leq \overline{\sigma}(G(j\omega))$$

In this relation, $\underline{\sigma}(G(j\omega))$ and $\overline{\sigma}(G(j\omega))$ are minimum and maximum singular values of $G(j\omega)$ at frequency ω. These are also called principal gains which are in turn used to compute a condition number as a ratio of the two. If the condition number is close enough to 1, it becomes easier to control the corresponding system.

Finally, the last definition of the term "gain" is a static gain that is the gain at $\omega = 0$, hence, $G(0)$. As the name suggests, it shows the ratio of the input and the output of a system under steady-state conditions.

The following transfer functions describe the relationships between the gas flow rate and the water temperature (from w_c to T) at 5 different operating conditions mentioned in Table 1.2:

$$G_{ol_{2,1_{e1}}}(s) = \frac{0.001392}{s^2 + 0.009606s + 3.121 \cdot 10^{-6}}$$

$$G_{ol_{2,1_{e2}}}(s) = \frac{0.00139}{s^2 + 0.01033s + 9.378 \cdot 10^{-6}}$$

$$G_{ol_{2,1_{e3}}}(s) = \frac{0.001389}{s^2 + 0.009978s + 6.258 \cdot 10^{-6}}$$

$$G_{ol_{2,1_{e4}}}(s) = \frac{0.001388}{s^2 + 0.01017s + 7.835 \cdot 10^{-6}}$$

$$G_{ol_{2,1_{e5}}}(s) = \frac{0.001393}{s^2 + 0.01031s + 9.351 \cdot 10^{-6}}$$

In Table 1.4 you can find the static gains of the aforementioned open-loop transfer functions.

Operating points	Static gains
e1	446.0109
e2	296.3753
e3	221.9559
e4	177.1538
e5	148.9680

Table 1.4: Static gains (from w_c to T) at 5 operating points

Note that the static gain decreases as the flow rate $\overline{w}$ increases.

1.3.3. Step response and Bode diagram

As a MIMO system, through the system's simulator we can demonstrate step responses from each of the 3 inputs to its 2 outputs as shown below:

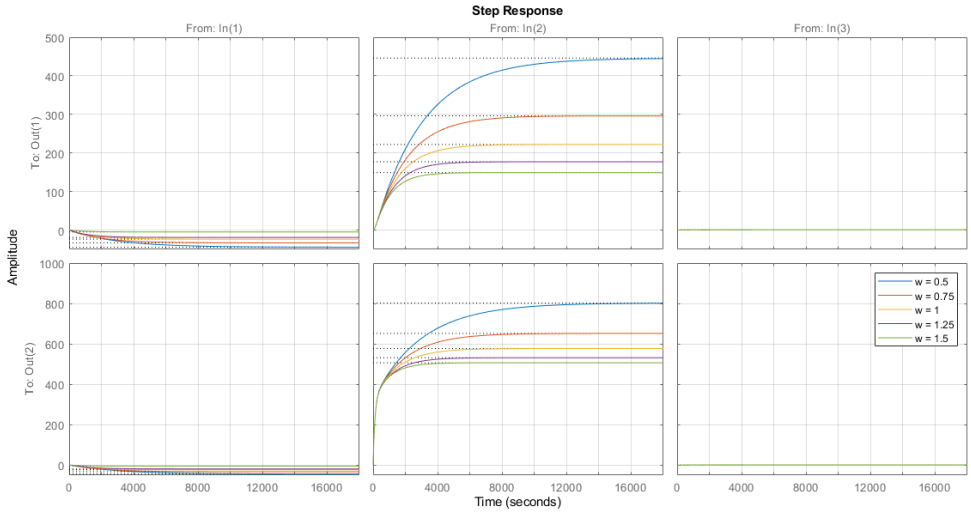

Figure 1.6: Step response of the thermo-hydraulic system at different operating points

It is clear from Figure 1.6, Bode diagrams of the transfer functions between w_c to T are different, mainly at low frequencies in different operating points, as already been stated in the analysis of the poles and gains.

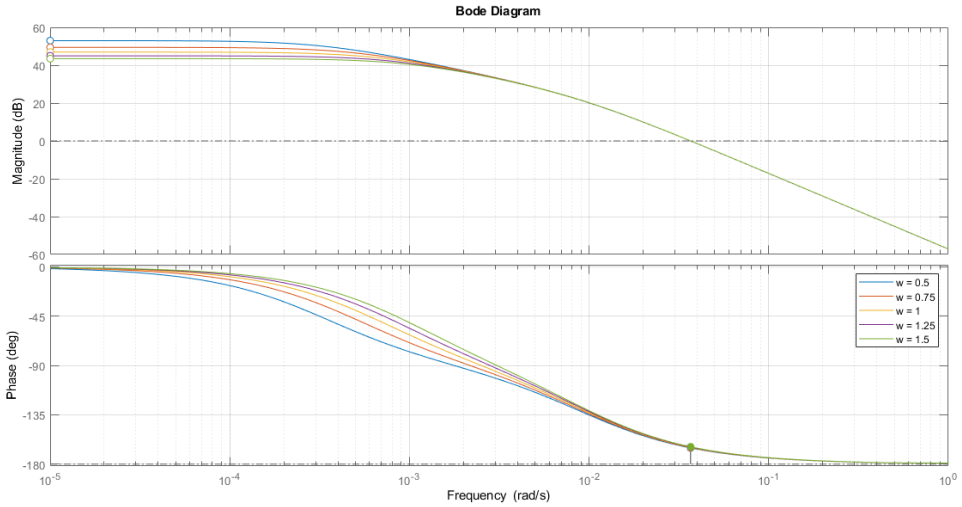

Figure 1.17: Bode plots of the three mentioned equilibrium points

1.4. Summary

We start by introducing a thermo-hydraulic system description in Section 1.1 and stated the system with the help of differential equations along with its parameters, its inputs and states. Later in Section 1.2, we determined an equilibrium point (later to be 5) that will later on be used to design controllers, after which in the following chapters will be tested on the non-linear system working at different operating conditions. The section covers state trajectories too, which was followed by linearization of it around the chosen operating point. Moreover, a state-space representation and transfer function of the linearized system are given, which helped us to determine some characteristics of the system, such as eigenvalues, static gains, step responses and Bode plots in Section 1.3.

2 Control Design

In this chapter, the linearized thermo-hydraulic system at $\bar{w} = 1$ is firstly used to design a PI controller. This controller is then used to regulate the system at different operating points. Later the control is realized by an LQ controller for the same system condition. Notice that in LQ it is initially assumed that the two states (T and T_m) are known. Later on, in another scenario the states will be estimated using Kalman Filter in the LQG control design. Additionally, H_2 and H_∞ controllers will be synthesized too. Finally, we propose a backtepping controller that is based on the Lyapunov stability theorem.

2.1. PI controllers

One of the most commonly used controllers in industry is a PI (proportional plus integral) controller, which lacks the derivative action of PID systems. As the name suggests, it is a type of controller that combines proportional and integral control actions making it a suitable tool for zero-error tracking. The PI controllers are mathematically illustrated by the following equation:

$$u(t) = K_c\left(e(t) + \frac{1}{T_i}\int e(t)dt\right)$$

where $u(t)$ is the controller output, K_c is the controller gain, T_i is the integral time, and $e(t)$ is the error signal.

Here we control the linearized system around the equilibrium point we discussed in Section 1.2 ($\bar{w} = 1$) by a PI controller. The controller ensures zero-error tracking for constant reference signals and disturbances (w).

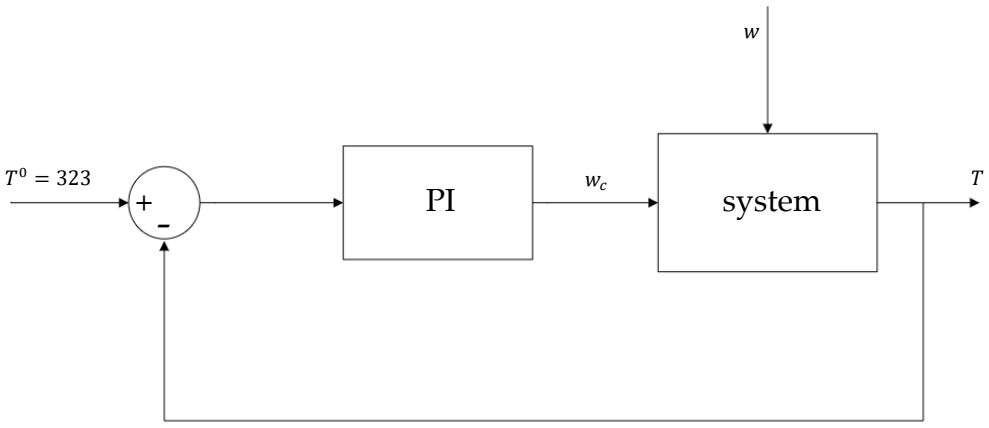

Figure 2.1: Block diagram of a closed-loop system

The goal of the analysis is to study the rejection properties of the system in front of load variations, that is steps of the load flow rate w. The load flow rate w in Figure 2.1 is moved in all the operating range from 0.5 to 1.5 over 20000 time units and is given as follows:

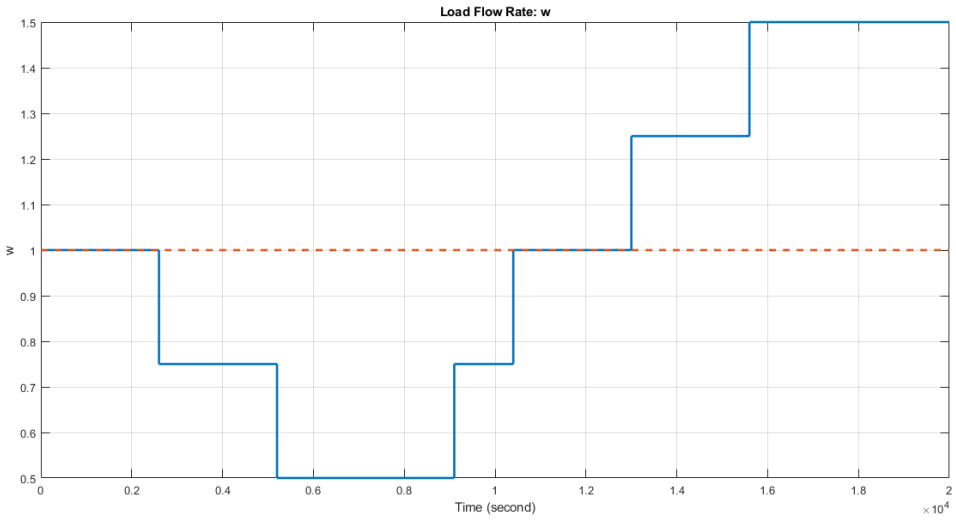

Figure 2.2: Load flow rate w

Now recall that the eigenvalues, thus the poles, of the linearized plant are -0.0007 and -0.0093 around the central operating condition ($\bar{w} = 1$) as shown in Table 1.3. Since we do not need any means, e.g., pole placement, to stabilize the system, let's move on synthesizing the PI regulator.

Consider the following open-loop transfer function from w_c to T:

$$G_{ol_{1,2}}(s) = \frac{0.001389}{s^2 + 0.009978s + 6.258 \cdot 10^{-6}}$$

To regulate the system, we use MATLAB's Control System Designer application. This application lets one design compensators for SISO systems. This is realized by graphical interactions with Bode plots or root locus of the open-loop system. The controller we want to design has a pole (integrator) at the origin and a real zero at $-a_{PI}$, and takes the following form:

$$R_{PI}(s) = K_{PI}\frac{(s + a_{PI})}{s}$$

Note that when we design a controller using Root Locus, we are allowed to move PI controller's zero ($-a_{PI}$) or the overall gain (K_{PI}) around the s-plane. In the design process, we neglect specific requirements, such as percent overshoot, settling or rise time, phase and gain margin and bandwidth. Nevertheless, the controller structure ensures that there is zero steady state error and that the system is robust to external disturbances.

The root locus method results in the following PI controller with real zero at -0.001198 and an overall gain of 0.018134:

$$R_{PI}(s) = 0.018134\frac{(s + 0.001198)}{s}$$

We implement the controller in Simulink as follows:

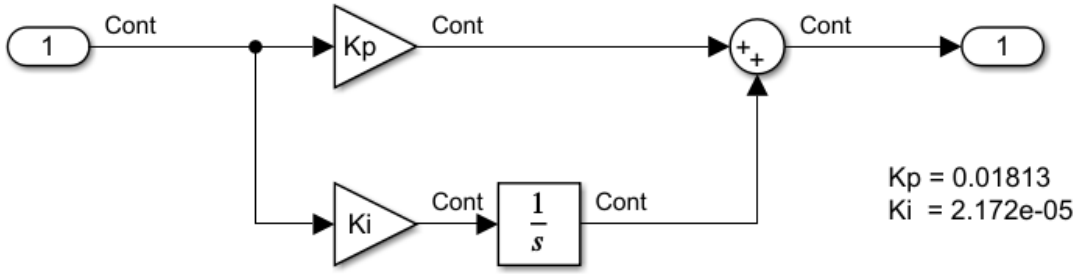

Figure 2.3: PI controller

After simulating the closed-loop system with the PI controller in the presence of the load flow rate shown in Figure 2.2, the water temperature response of the non-linear thermo-hydraulic plant at different operating points becomes:

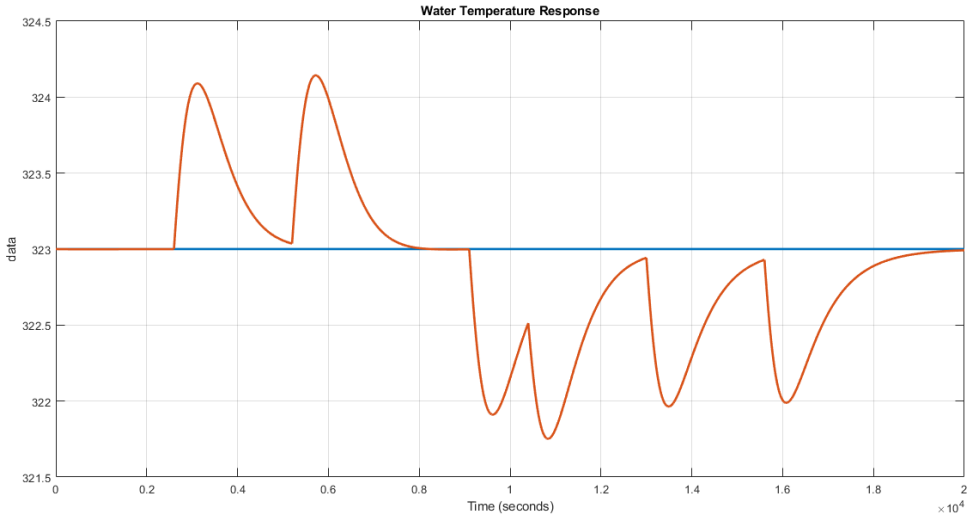

Figure 2.4: Water temperature response with PI control

As can be seen from Figure 2.4, the response is not accompanied by an oscillatory behavior. Most importantly, the settling time is extremely large, roughly 5000 time units. However, the response varies from 321.7515 to 324.1434, from which one can conclude that the PI controller designed and implemented for the system help it be stable around its reference value at $T^0 = 323$.

To assess the stability of a closed-loop system we use Nyquist criterion, root locus or Bode diagrams. All these three methods make use of the open-loop transfer function (or loop transfer function) $L(s)$. In this sense, the gain margin and the phase margin are useful to determine important properties of the feedback systems, and they are the measure of the control system's stability.

Let's compute the loop transfer function and the associated gain and phase margins.

$$L(s) = R_{PI}(s) \cdot G_{ol_{1,2}}(s) = \frac{2.519 \cdot 10^{-5}\, s \;+\; 3.018 \cdot 10^{-8}}{s^3 \;+\; 0.009978\, s^2 \;+\; 6.258 \cdot 10^{-6}\, s}$$

The corresponding Bode plot is given as shown below:

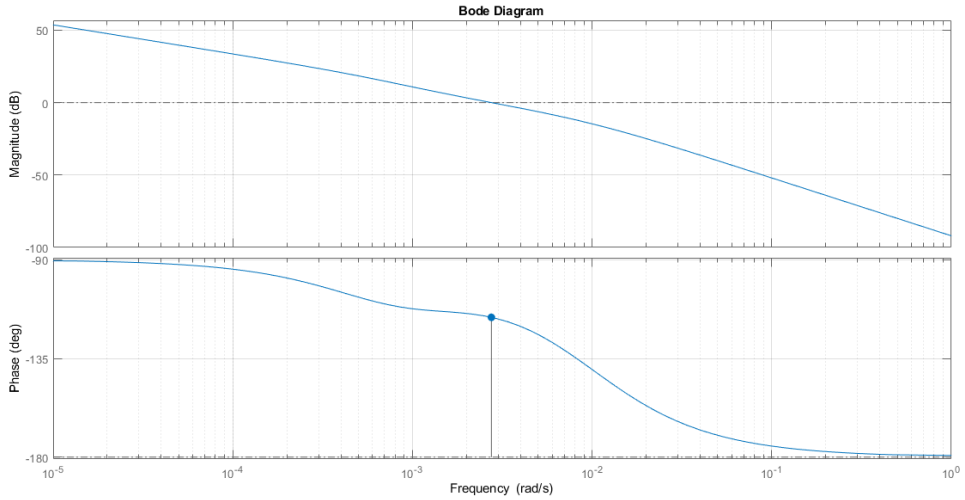

Figure 2.5: Bode plot of the loop transfer function

We notice that at 0.00275 rad/s the phase margin can be pointed and that is 63.7°. Additionally, the associated gain margin is infinite. The quite large value of the phase margin guarantees some robustness properties of the closed-loop system, that behaves well also for operating points far from the nominal operating condition where the PI has been tuned.

The phase and gain margins measure the distance from the Nyquist plot of the loop transfer function $L(s)$ to the point -1 at specified frequencies. The inverse of the gain margin is the distance from the critical point -1 to the intersection of $L(j\omega)$ with the real axis. As can be seen, the loop transfer function does not intersect the real axis, thus an infinite gain margin. On the other hand, the phase margin is the radian of the segment from (-1, 0) to the intersection point of $L(j\omega)$ with the unit circle. See the figure below:

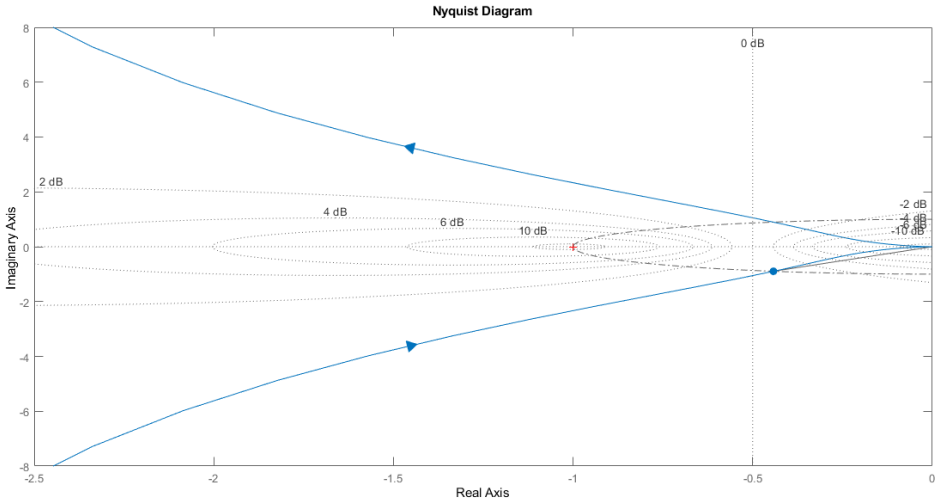

Figure 2.6: Nyquist plot of the loop transfer function

As far as $L(s)$ is concerned, if there is one or more integrators in its transfer function, $|L(s)|$ will be high at low frequencies, which in turn guarantees asymptotic zero-error for constant reference signals and disturbances. Note that there is an integrator in $L(s)$ in our case as well.

While designing a regulator, it is always advisable to consider the following:

1. Phase margin should be large.
2. Crossover frequency should be large, which guarantees satisfactory speed of response, attenuation of disturbance signals, and tracking the reference. On the other hand, to attenuate the measurement noise, the newly designed controller introduces a smaller crossover frequency.
3. Gain margin should be high. The Bode diagrams of both $G_{ol_{1,2}}(s)$ and $L(s)$ show that the gain margins for both cases are infinite. However, an infinite gain margin does not always mean that the system is highly stable. To elaborate this discussion, let's introduce the sensitivity function of the given system:

$$S(s) = \frac{1}{R_{PI}(s) \cdot G_{ol_{1,2}}(s)}$$

Now we can plot this transfer function across the entire spectrum using the Bode plot and determine where its maximum sensitivity is. It turns out that it is around

1.68 dB, which is 1.3302 in decimals. Notice that we usually want a maximum peak sensitivity of 1.3 to 2.

You can also see the other output's (the metal temperature T_m) response in Figure 2.7 in the presence of the varying load flow rate w. It is obvious that the step response at different operating points results in large deviation from its reference value, $T_m^0 = 363$. It is, however, interesting to note that the form of the response is quite different at different operating points, which is obvious in view of the nonlinearity of the system.

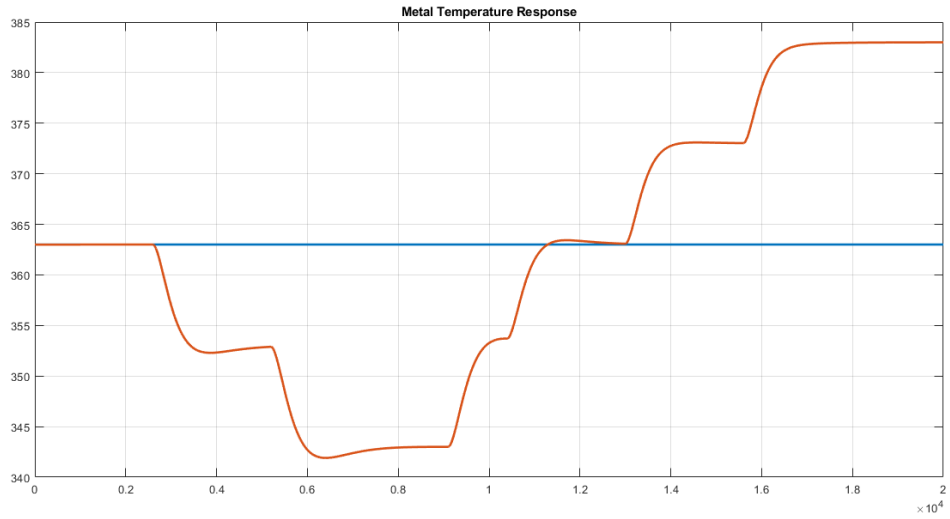

Figure 2.7: Metal temperature with PI control

2.2. LQ control with integral action

In this section of the chapter, we design an LQ controller guaranteeing asymptotic zero error regulation for constant references. To this end, we augment the linearized system to later implement an integrator to control the water temperature. Before computing the enlarged system, let us have a look at some theory.

It is, as in the case of SISO systems, possible to guarantee zero steady-state error in MIMO systems by adding an integral action in each error signal as shown in Figure 2.8. The system obtained this way is robust, in the sense that for given constant set-points, the unique state-space condition is as follows:

$$e_i = 0, i = 1, \dots, p.$$

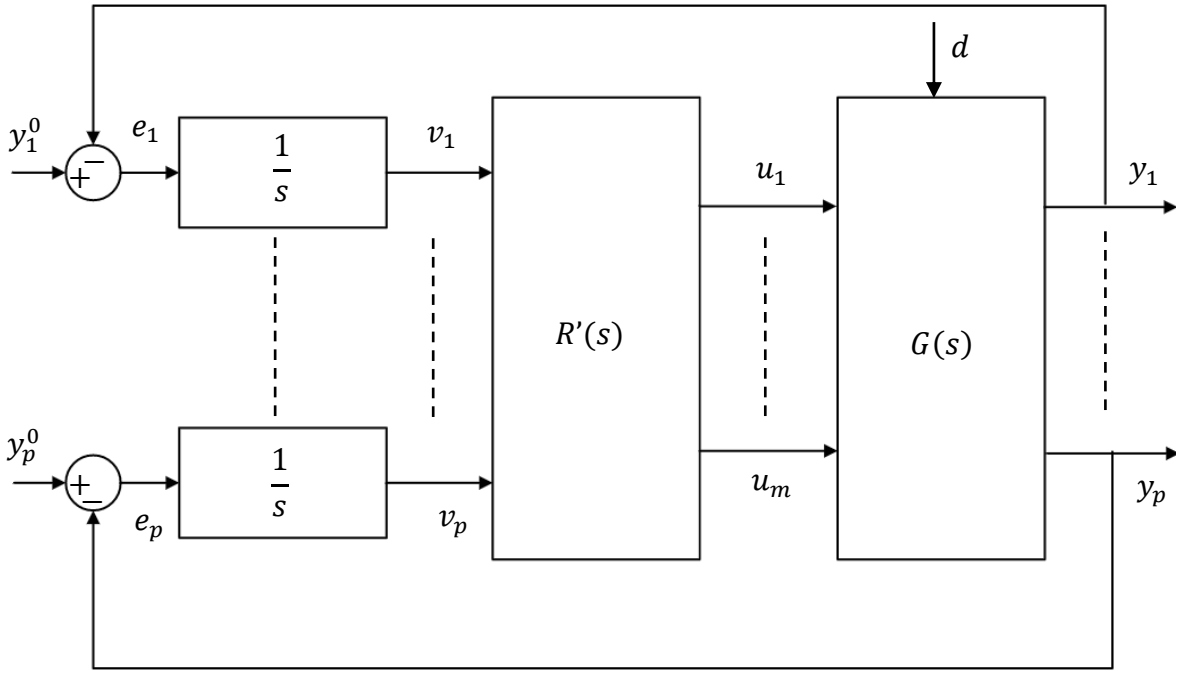

Figure 2.8: Integral action on the error signal in MIMO systems

Although the error requirement is met, the regulator $R'(s)$ synthesis still needs to be designed. Consider the following system under control:

$$\dot{x}(t) = Ax(t) + Bu(t) + Md$$

$$y(t) = Cx(t) + Nd$$

with $x \epsilon R^n, u \epsilon R^m, y \epsilon R^p$, and $d \epsilon R^r$. d is a constant disturbance that acts on the states and the outputs. Recall the zero steady-state error requirement: $y^0 = y$ for any y^0 and d. At the steady state it must hold that

$$0 = A\bar{x} + B\bar{u} + Md$$

$$y^0 = C\bar{x} + Nd$$

These expressions can be rewritten as:

$$\begin{bmatrix} A & B \\ C & 0 \end{bmatrix} \begin{bmatrix} \bar{x} \\ \bar{u} \end{bmatrix} = \begin{bmatrix} 0 & -M \\ I & -N \end{bmatrix} \begin{bmatrix} y^0 \\ d \end{bmatrix}$$

The first matrix in the left side of the equation is denoted as Σ and $\Sigma \epsilon R^{n+p,n+m}$. From here we get the following conditions to guarantee that there is one pair $(\bar{x}, \bar{u})$ that satisfies the previously mentioned relation for any constant y^0 and d:

1. $p \leq m$.
2. $rank(\Sigma) = n + p$

The first condition requires that the number of control variables is greater or equal to that of the system outputs (at least as many inputs as outputs), whereas the second condition is to guarantee that there is no derivative action, or any invariant zeros in $s = 0$.

Let us have a look at Figure 2.8 and write the integrators in state variables:

$$\dot{v}(t) = e(t) = y^0 - y(t) = y^0 - Cx(t) - Nd$$

Thus, the enlarged system that consists of the original system and integrators can be described as follows:

$$\begin{bmatrix}\dot{x}(t)\\ \dot{v}(t)\end{bmatrix} = \begin{bmatrix} A & 0 \\ -C & 0 \end{bmatrix}\begin{bmatrix}x(t)\\ v(t)\end{bmatrix} + \begin{bmatrix}B\\ 0\end{bmatrix}u(t) + \begin{bmatrix} 0 & M \\ I & -N \end{bmatrix}\begin{bmatrix}y^0\\ d\end{bmatrix}$$

$$v(t) = \begin{bmatrix} 0 & I \end{bmatrix}\begin{bmatrix}x(t)\\ v(t)\end{bmatrix}$$

From these equations of the enlarged system, we define:

$$\tilde{A} = \begin{bmatrix} A & 0 \\ -C & 0 \end{bmatrix}, \quad \tilde{B} = \begin{bmatrix}B\\ 0\end{bmatrix}, \qquad \tilde{C} = \begin{bmatrix} 0 & I \end{bmatrix}$$

To synthesize the regulator ($R'(s)$), the pair $(\tilde{A}, \tilde{C})$ must be observable or detectable and the pair $(\tilde{A}, \tilde{B})$ must be reachable or stabilizable. These two pairs meet this requirement if and only if the original pair (A, C) is observable and (A, B) is reachable and the system does not contain any invariant zero in $s = 0$ (no derivative action).

Let us consider the thermo-hydraulic plant and augment it. To design and implement a LQ controller for our enlarged system with an integrator, we need to check two conditions first.

1. $p \leq m$. This requirement is met since both the number of control variables (w_c) and the number of controlled outputs (T) are 1. Therefore, the water temperature can be controlled.
2. $rank(\Sigma) = n + p$, This condition helps us decide if the system has invariant zeros. The system matrix Σ is:

$$\Sigma = \begin{bmatrix} 0.0011 & -0.0004 & 0.0167 & 0 \\ -0.0088 & 0.0088 & 0 & -3.1422 \\ 1.0000 & 0 & 0 & 0 \end{bmatrix}$$

Since the $rank(\Sigma) = 2 + 1 = 3$ (fully ranked), we conclude that there is no derivative action.

Let us now enlarge the system by adding an integrator to the loop from w_c to T, as shown in Figure 2.9:

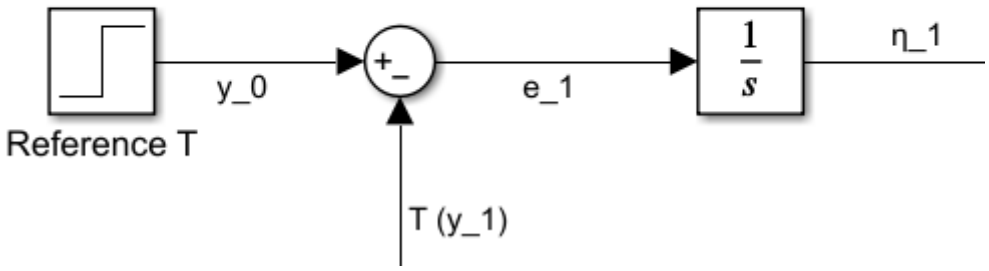

Figure 2.9: Integrators of the enlarged system

We denote the matrix C to correspond to y_1:

$$\dot{\eta_1} = e_1 = y_1^0 - y_1 = \delta y_1^0 - \delta y_1 = \delta y_1^0 - C\delta x$$

Thus, the enlarged system becomes:

$$\begin{bmatrix} \dot{\delta x} \\ \dot{\eta_1} \end{bmatrix} = \begin{bmatrix} A & \begin{bmatrix} 0 \\ 0 \end{bmatrix} \\ C & 0 \end{bmatrix} \begin{bmatrix} \delta x \\ \eta_1 \end{bmatrix} + \begin{bmatrix} B \\ 0 \end{bmatrix} \delta u + \begin{bmatrix} \begin{bmatrix} 0 \\ 0 \end{bmatrix} \\ 1 \end{bmatrix} \delta y_1^0$$

$$\dot{\tilde{x}} = \tilde{A}\tilde{x} + \tilde{B}\delta u + \tilde{M}\tilde{d}$$

Now let us design a state feedback control law for the enlarged system using LQ control after a brief introduction. Linear Quadratic (LQ) control approach is a popular method resulting from formulating the optimal control problem and solving it for linear systems and quadratic cost functions. Let us consider the following system with initial time at $t_0 = 0$ along with the performance index:

$$\dot{x}(t) = Ax(t) + Bu, \qquad x(0) = x_0$$

$$J(x_0, u(\cdot), 0) = \int_0^\infty (x^T(\tau)Qx(\tau) + u^T(\tau)Ru(\tau))d\tau$$

where the design parameters are $Q = Q' \geq 0$ and $R = R' > 0$. The infinite horizon Linear Quadratic control problem is obtained by minimizing the const function J with respect to u. If the pair (A, B) is reachable, the solution of the ordinary differential Riccati equation tends to a constant matrix $\bar{P} \geq 0$, that is in turn the solution to the algebraic Riccati equation as shown below:

$$0 = A^T\bar{P} + \bar{P}A + Q - \bar{P}BR^{-1}B^T\bar{P}$$

together with the control law:

$$u(t) = -R^{-1}B^T\bar{P}x(t) = -\bar{K}x(t), \qquad \bar{K} = R^{-1}B^T\bar{P}$$

The matrix Q can always be partitioned as $Q = C_q'C_q$, which is not necessarily unique. $\bar{P}$ is positive definite if and only if the pair (A, C_q) is observable.

We can summarize the two conditions to be checked before implementing LQ control:

1. The pair (A, B) is reachable
2. The pair (A, C_q) is observable

In the algebraic Riccati equation the matrices A and B are given, which are the enlarged system's matrices as shown earlier $(\tilde{A}, \tilde{B})$. Let us assume that the asymptotic solution to this equation, $\bar{P}$, is a 3x3 matrix:

$$\bar{P} = \begin{bmatrix} p_{11} & p_{12} & p_{13} \\ p_{21} & p_{22} & p_{23} \\ p_{31} & p_{32} & p_{33} \end{bmatrix} = P'$$

As far as the tuning parameters Q and R are concerned, the choice is non-trivial. These parameters are used to penalize the state variables and the control signal, i.e., the larger these values, the more you penalize the signals. Choosing a large value for R, we do not intend to use too much energy, which is called an expensive control strategy. However, smaller values of R indicate that one does not want to penalize the control signal, which is a cheap control strategy. The same can be interpreted for values of Q and its effect on the changes of states. Since there is always a trade-off between these two, we are going to keep Q as an identity matrix while modifying R:

$$Q = \begin{bmatrix} 1 & 0 & 0 \\ 0 & 1 & 0 \\ 0 & 0 & 1 \end{bmatrix} \qquad R = 0.1$$

We solve the algebraic Riccati equation using MATLAB's ***lqr*** command which computes the state-feedback control law $u(t) = -\bar{K}x(t)$ that minimizes the above-mentioned cost function. The resulting solution, $\bar{P}$, is as follows:

$$\bar{P} = 10^5 \cdot \begin{bmatrix} 1.4681 & 0.0001 & -0.0227 \\ 0.0001 & 0.0000 & -0.0000 \\ -0.0227 & -0.0000 & 0.0007 \end{bmatrix}$$

We can now get the gain matrix $\bar{K}$:

$$\begin{aligned} \bar{K} = [k_1 \quad k_2 \quad k_3] &= R^{-1}B'\bar{P} \\ &= 10 \cdot \begin{bmatrix} 0 \\ 3.1422 \\ 0 \end{bmatrix}^T \cdot 10^5 \cdot \begin{bmatrix} 1.4681 & 0.0001 & -0.0227 \\ 0.0001 & 0.0000 & -0.0000 \\ -0.0227 & -0.0000 & 0.0007 \end{bmatrix} \\ &= [204.9502 \quad 3.1686 \quad -3.1623] \end{aligned}$$

Recall that $\bar{K}$ corresponds to the enlarged system's gain, thus we need to partition it into two parts:

$$\bar{K}_x = [k_1 \quad k_2] = [204.9502 \quad 3.1686]$$

$$\bar{K}_{\eta_1} = [k_3] = [-3.1623]$$

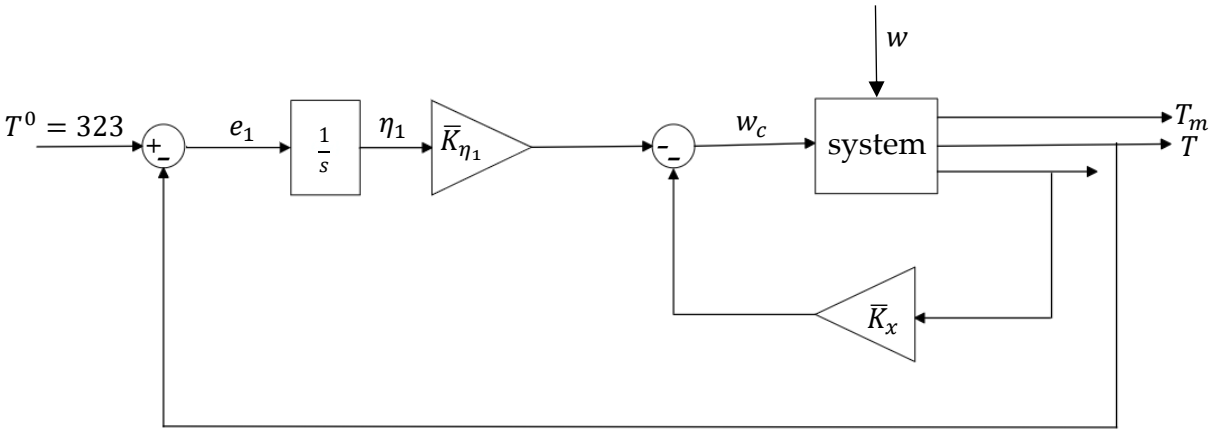

Figure 2.10: LQ control on the enlarged system

After implementing the block diagram shown in Figure 2.9 in Simulink with the same experiment of load flow rate (w) as in the previous simulations, we end up with the following water temperature response:

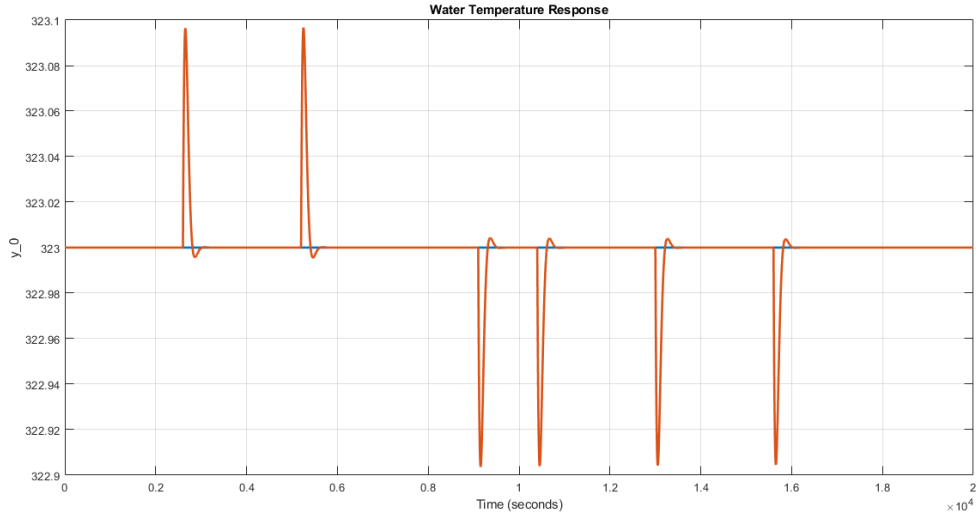

Figure 2.11: Water Temperature Response with LQ

To better analyze the system response, let us reduce the interval between two step inputs of the disturbance w and run the simulation again:

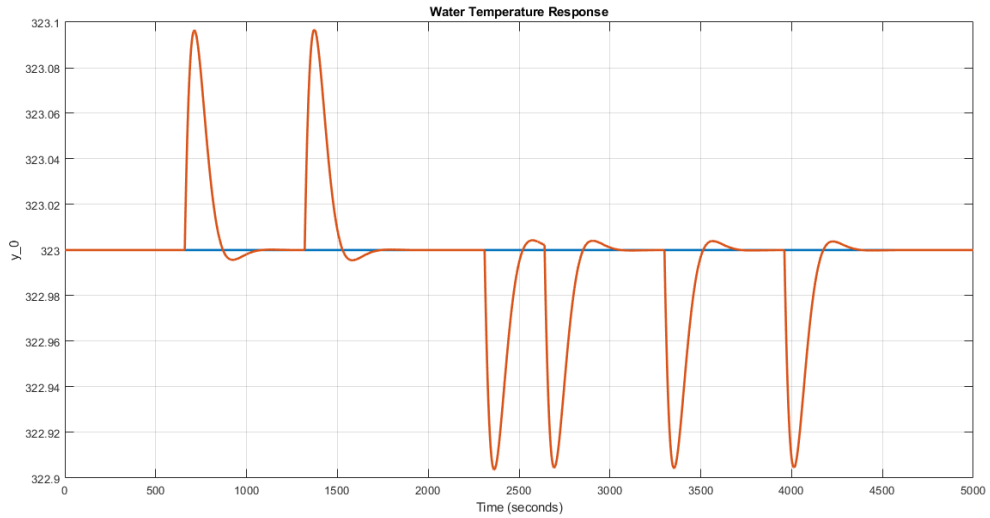

Figure 2.12: Water Temperature Response with LQ

As can be seen from Figure 2.11, the water temperature response is not oscillatory. Furthermore, the settling time in this case is relatively small, at 600 time units, which is 8 times smaller than that of the PI control. In addition to that, the response is associated with peaks at 322.9036 and 323.0967, which is negligible comparing to the reference value at $T^0 = 323$. Note that the goal of zero-error tracking is met with LQ control with some more advantages.

Speaking of LQ control, it is worth mentioning the control signal too. In Figure 2.13 you can see that the control action is not volatile with the assigned value of R matrix, which is 0.1 in this example.

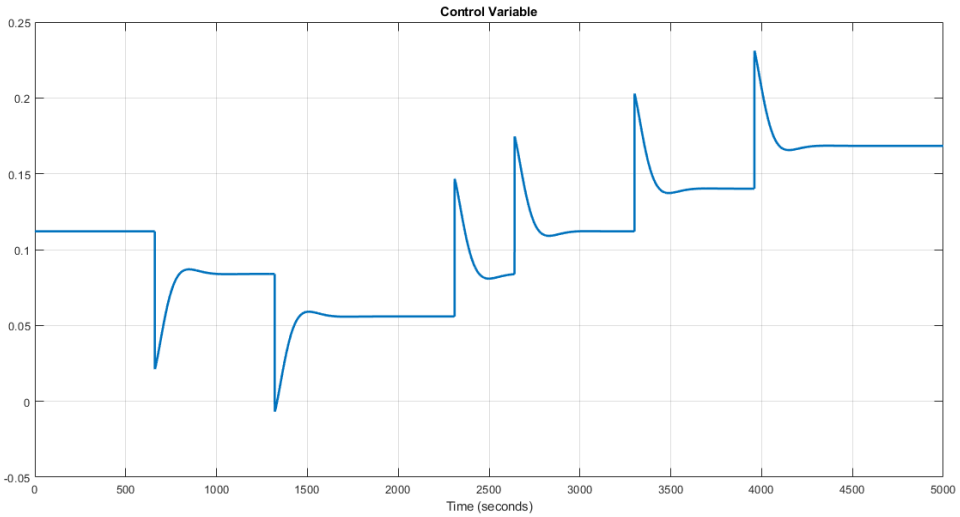

Figure 2.13: Control variable with LQ

Finally, one can find the metal temperature response of the system, that is the other state of the thermo-hydraulic system, in Figure 2.14 below. Note that due the non-linearity of the system, the response is different at different operating points as it was the case for PI control structure too.

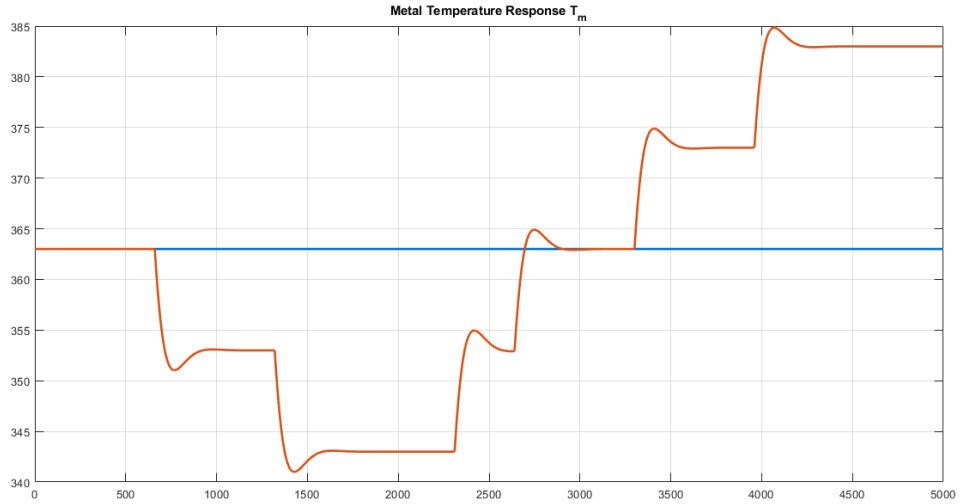

Figure 2.14: Metal temperature response with LQ

2.3. Pole Placement

In this section we now design a state feedback control law with pole placement.

Let us consider the continuous-time system given below:

$$\dot{x}(t) = Ax(t) + Bu(t)$$

$$y(t) = Cx(t) + Du(t)$$

with $x \epsilon R^n, u \epsilon R^m, y \epsilon R^p$. Here we assume the state x to be measurable and that the algebraic control law holds:

$$u(t) = -Kx(t) + v(t), \quad K \epsilon R^{m,n}, \quad v \epsilon R^m$$

Note that the matrix K is the pole-placement gain and is responsible for stabilization, while $v(t)$ is an input signal possibly from an outer loop which can be used to design external loops. The resulting closed-loop system, by combining the state equation and the control law, becomes:

$$\dot{x}(t) = (A - BK)x(t) + Bv(t)$$

We can conclude that the pole placement problem is to compute the matrix K so that we can arbitrarily assign the eigenvalues of $(A - BK)$.

From theory we know that the necessary and sufficient condition for a pole-placement problem is that the system is reachable. In other words, we first need to

check if the pair (A, B) of the loop from w_c to T is reachable before introducing the state-feedback control law by means of pole-placement.

The reachability matrix M_r for a n-state system is given as:

$$M_r = [B, \ AB, \dots, A^{n-1}B]$$

For the system to be fully reachable, the matrix M_r should have a full rank. Given the original linearized thermo-hydraulic plant, we obtain the following reachability matrix:

$$M_r = \begin{bmatrix} 0 & 0.0014 \\ 3.1422 & -0.0277 \end{bmatrix}$$

As it can be seen, the rank of the aforementioned matrix is 2, thus fully ranked.

Since the linearized system is fully reachable, we can implement a state-feedback law using pole-placement. We continue by defining the matrix K. In theory the solution to the pole-placement theory for single input systems is computed by the Ackermann's formula. However, in practice a more convenient way is used to compute the matrix K, for example, in MATLAB there is a function called ***place***, which can be used also for multi input systems and uses all the available inputs, and guarantees robustness for the system under consideration.

In our case, we want to relocate poles from (-0.0007, -0.0093) to (-0.1, -0.1) using MATLAB's built-in function ***place***. The resulting matrix K is a 1x2 matrix and is as follows:

$$K = [7.0375 \quad 0.0605\,]$$

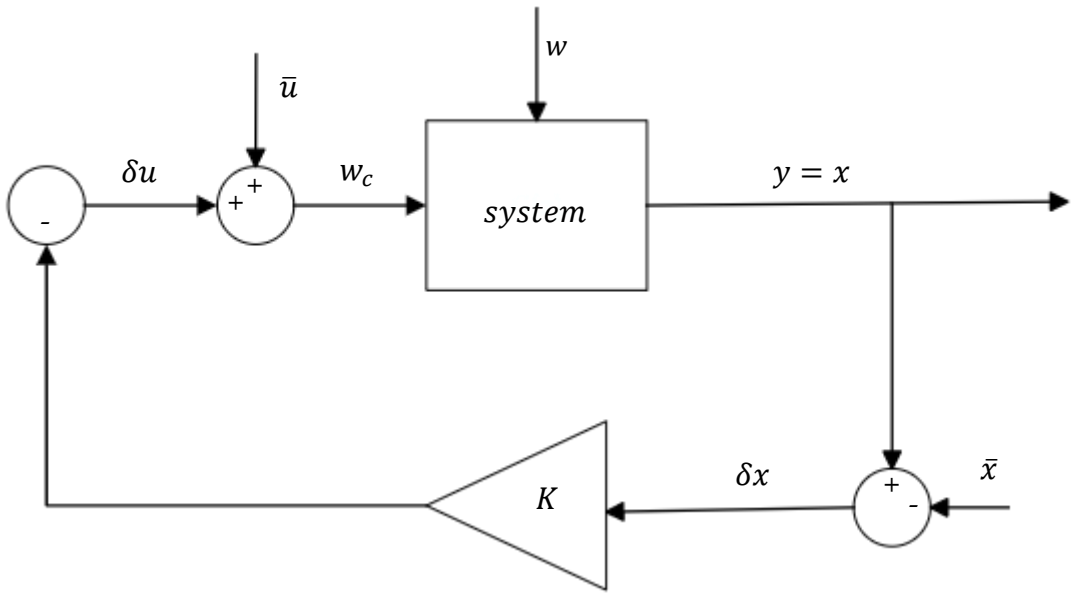

Figure 2.15: Pole-placement implementation

After implementing the state-feedback control structure shown in Figure 2.15 on Simulink, the output response of the thermo-hydraulic system becomes:

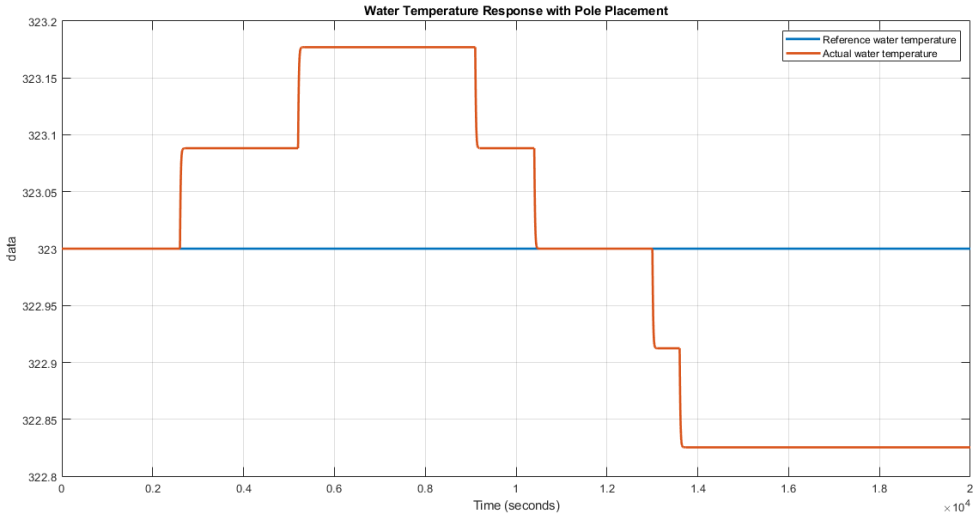

Figure 2.16: Water temperature response with pole placement

Note that here we repeat the same experiment that has been carried out in the previous section concerning the flow rate disturbance, thus the load flow rate w corresponds to the signal in Figure 2.2. As can be seen from Figure 2.16, the output response does not meet the goal of zero steady-state error. It is also worth mentioning that water temperature varies from 322.8254 to 323.1770 over the simulation time. In general, the system behaves not so well for operating points far from the nominal operating condition where the original pole-placement was constructed. To tackle this problem, let us add an integrator to the loop associated with the control variable w_c to enlarge the system. Afterwards, we can implement the pole-placement technique to the enlarged system.

Consider the enlarged system in Section 2.2. Indeed, the pole-placement method uses the same scheme of enlarged system, but to compute different gains from the infinite LQ control.

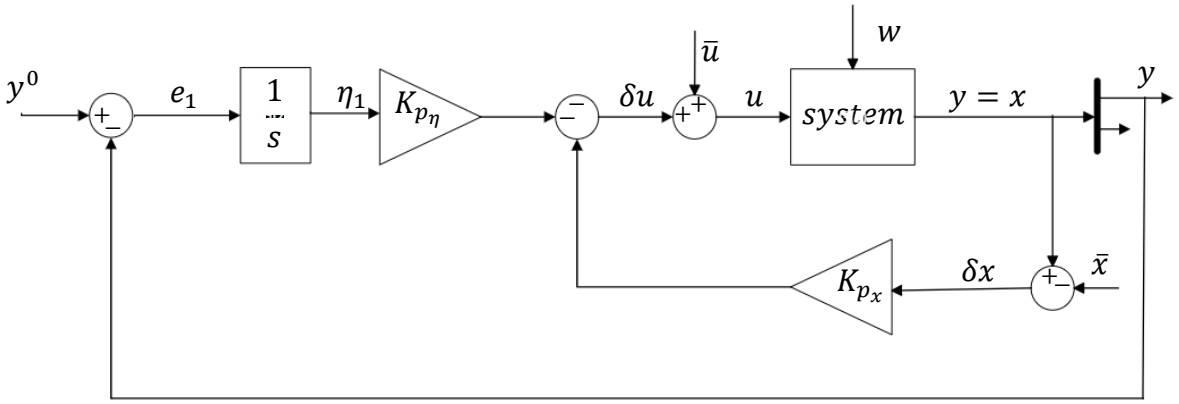

Figure 2.17: Enlarged system with pole placement

From Figure 2.17, it becomes clear that:

$$\dot{\eta_1} = e_1 = y^0 - \delta x_1$$

Considering the original system and the previous expression, the enlarged system is defined as follows:

$$\begin{bmatrix} \delta\dot{x}_1 \\ \delta\dot{x}_2 \\ \dot{\eta}_1 \end{bmatrix} = \begin{bmatrix} A & 0_{2x1} \\ [-1 \;\; 0] & 0 \end{bmatrix} \begin{bmatrix} \delta x_1 \\ \delta x_2 \\ \eta_1 \end{bmatrix} + \begin{bmatrix} B \\ 0 \end{bmatrix} u + \begin{bmatrix} 0_{2x1} \\ 1 \end{bmatrix} y^0$$

$$\dot{\tilde{x}} = \tilde{A}\tilde{x} + \tilde{B}\delta u + \tilde{M}y^0$$

As before, we use MATLAB's ***place*** function to calculate the pole placement gain matrix $K_{en_{pp}}$, by relocating the poles to (-0.01, -0.01, -0.02). This matrix will later be partitioned into two matrices to be implemented in the simulation.

$$K_{en_{pp}} = [0.3308 \quad 0.0096 \quad -0.0014]$$

$$K_{en_{pp}} = \begin{bmatrix} K_{p_\eta} & K_{p_x} \end{bmatrix}, \qquad K_{p_x} = [0.3308 \quad 0.0096], \qquad K_{p_\eta} = -0.0014$$

The same shape of the load flow rate *w* as an external disturbance shown in Figure 2.2 has been used in this setup with smaller intervals between steps so that one can analyze the response better. The simulation results show that the output response, due to the choice of the poles, is faster than the control methods shown previously. At different operating points, it takes almost 500 time units for the

water temperature to get to its desired state ensuring the zero-error state condition. See Figure 2.18 below.

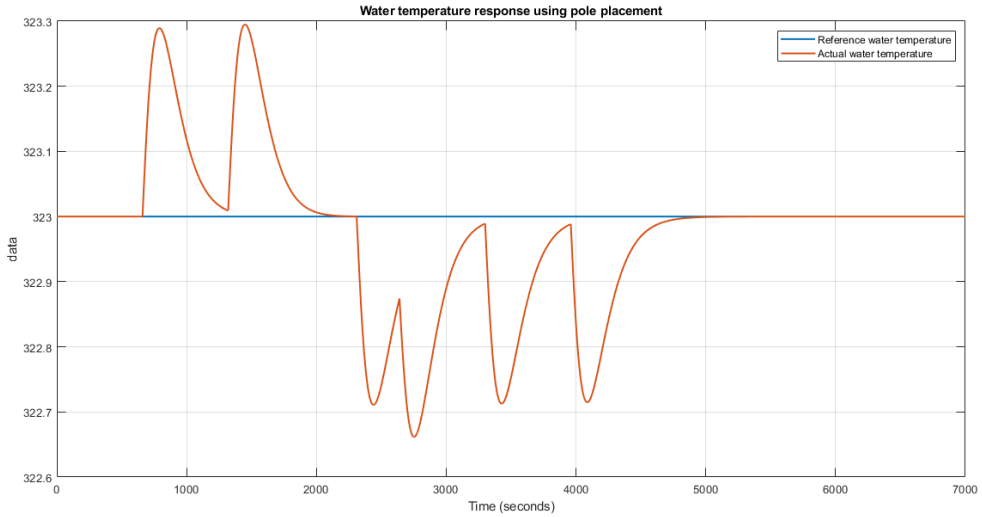

Figure 2.18: Enlarged system's water temperature using Pole Placement

Note that in pole placement, a good choice of relocations of the poles should be put forward, so that the input control variable (w_c) does not take large values. Therefore, this assumption is met with the given choice of poles, see Figure 2.19:

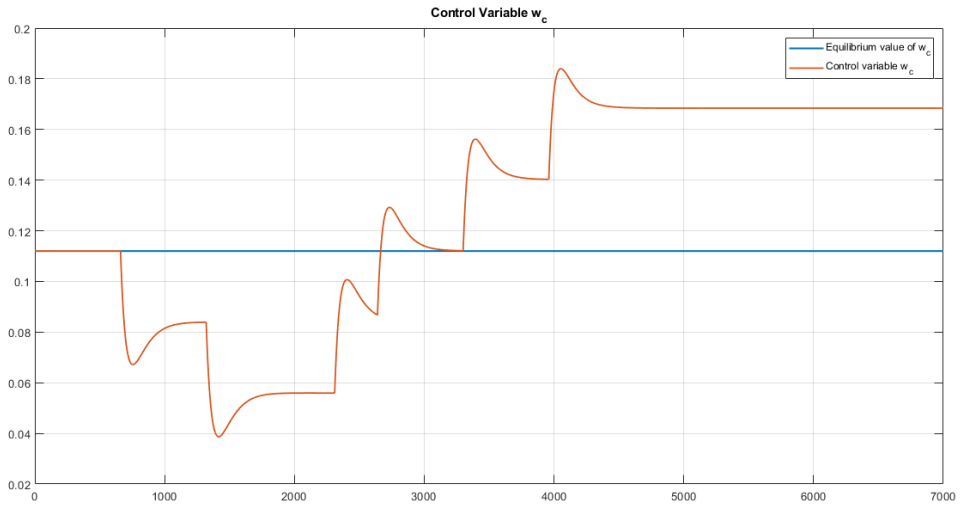

Figure 2.19: Enlarged system's control variable w_c using Pole Placement

2.4. LQG control

This section presents an LQG controller design process to reflect the above-given control considerations. The LQG, which stands for the Linear Quadratic Gaussian, control is a combination of the LQ control and a Kalman filter. The latter is used to estimate the states of a process when it is affected by stochastic noises.

In the LQG control, the system is assumed to have the following form:

$$\dot{x}(t) = Ax(t) + Bu(t) + v_x(t)$$

$$y(t) = Cx(t) + v_y(t)$$

Here $v_x(t)$ and $v_y(t)$ are the noises. Notice that these variables and the initial state $x(0)$ satisfy all the necessary assumptions to derive the Kalman filter. For the system above, the optimization goal is to minimize the following cost function when the state x is non-measurable:

$$J = \lim_{T\to\infty} \frac{1}{T} E\left[\int_0^T \left(x^T(t)Qx(t) + u^T(t)Ru(t)\right)dt\right]$$

In this formulation the expected value operator should be used due to the stochastic noises which in turn make x and u stochastic processes in the closed loop as well. Having considered suitable assumptions, asymptotic stability is guaranteed in the LQG control so that the processes x and u are stationary stochastic processes. Thus, the aforementioned cost function can be written as:

$$J = E[x^T(t)Qx(t) + u^T(t)Ru(t)]$$

The solution to the LQG control problem is obtained after considering certain assumptions. We, first, assume that the hypotheses required for the infinite horizon Linear Quadratic control are satisfied. These are the observability of the pair (A, C_q), where $Q = C_q^T C_q$, and the reachability of the pair (A, B). Moreover, another assumption concerning the Kalman predictor should be made too, that is, the reachability of the pair (A, B_q), where $\tilde{Q} = B_q B_q^T$, and the observability of the pair (A, C). The separation theorem allows us to solve the LQG problem. For this to occur, we follow the steps below:

1. Compute $\bar{L}$ and $\hat{x}$, i.e., the observer gain and the corresponding optimal state estimate, by applying the asymptotic Kalman filter
2. Compute $\bar{K}$, the control gain, by solving the LQ control problem with measurable state
3. Apply the control law

$$u(t) = -\bar{K}\hat{x}(t)$$

Consider the following scheme of LQG control:

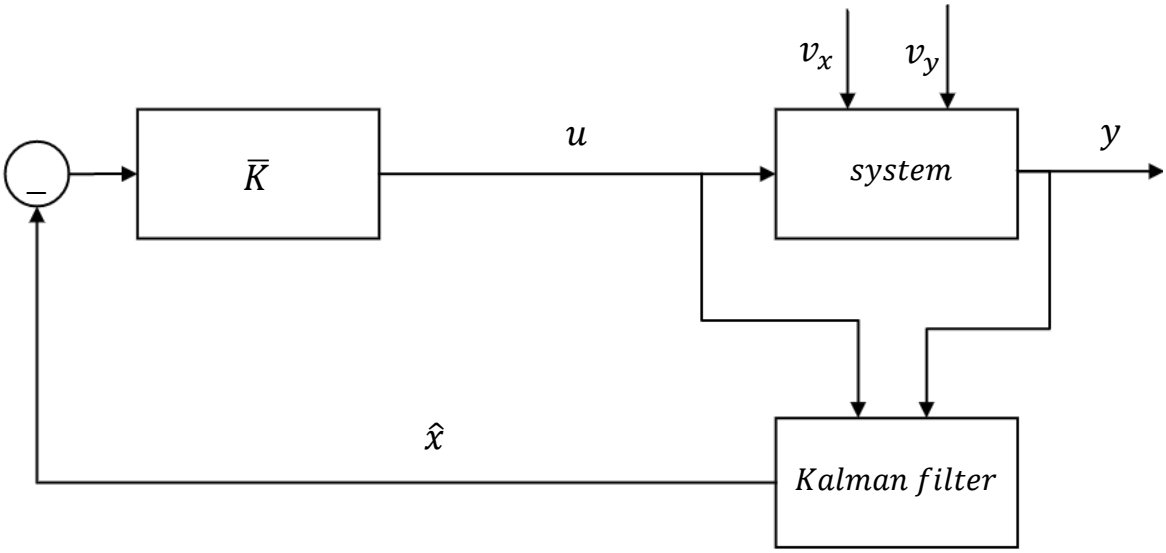

Figure 2.20: LQG control scheme

The constructed regulator takes the following dynamics:

$$\dot{\hat{x}}(t) = A\hat{x}(t) + Bu(t) + \bar{L}[y(t) - C\hat{x}(t)]$$

$$u(t) = -\bar{K}\hat{x}(t)$$

Using Laplace transforms and assuming that $\hat{x}(0) = 0$:

$$s\hat{X}(s) = (A - \bar{L}C)\hat{X}(s) - B\bar{K}\hat{X}(s) + \bar{L}Y(s)$$

$$\hat{X}(s) = (sI - (A - \bar{L}C - B\bar{K}))^{-1}\bar{L}Y(s)$$

The corresponding control input takes the following form:

$$U(s) = -\bar{K}\big(sI - (A - \bar{L}C - B\bar{K})\big)^{-1}\bar{L}Y(s) = -R(s)Y(s)$$

where

$$R(s) = \bar{K}\big(sI - (A - \bar{L}C - B\bar{K})\big)^{-1}\bar{L}$$

By the way of conclusion, it can be shown that the eigenvalues of the resulting closed-loop system are those of $(A - \bar{L}C)$ and $(A - B\bar{K})$.

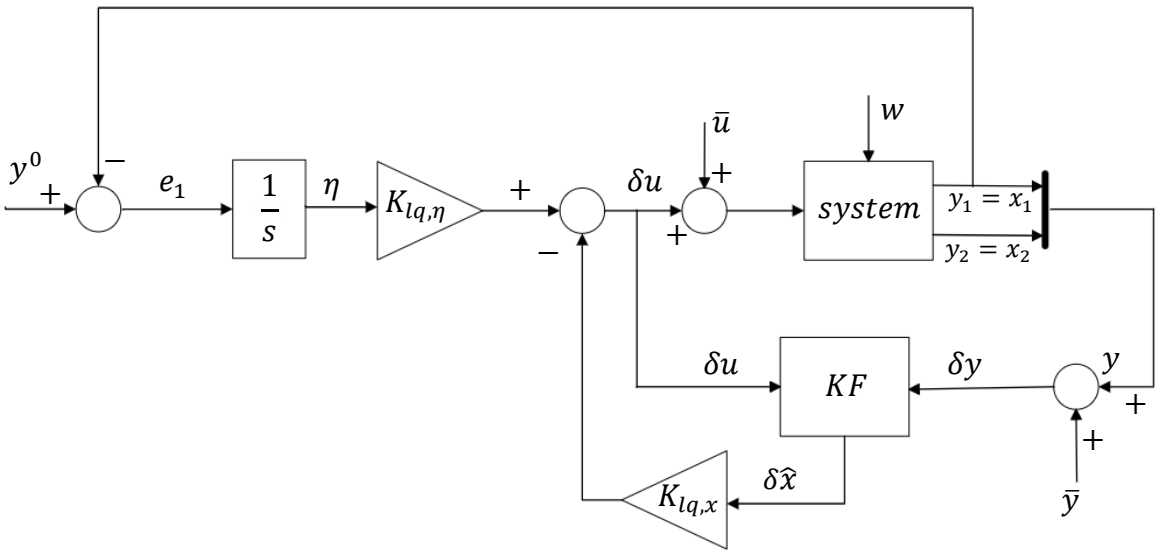

Figure 2.21: LQG control scheme of the thermo-hydraulic system

Let us assume that we can measure both outputs (the temperatures of the water and the metal) of the thermo-hydraulic plant, as shown in Figure 2.21. To design and implement a Kalman Filter to estimate the two states of this system, consider the following system:

$$\delta\dot{x} = A\,\delta x + B\,\delta u + v_x$$

$$\delta y = C_y\,\delta x + v_y$$

where $v_x \sim WGN(0, Q_{kf})$ and $v_y = WGN(0, R_{kf})$. Q_{kf} and R_{kf} are chosen as follows:

$$Q_{kf} = \begin{bmatrix} 1 & 0 \\ 0 & 1 \end{bmatrix} \qquad R_{kf} = 0.1$$

In the choice of Q_{kf}, different values are taken over the diagonal of the matrix to penalize the models of the states to represent which of them are most reliable. However, in this example, these values are the same. On the other hand, $R_{kf} = 0.1$ to give more trust to the measurements than the linearized model.

As mentioned above, the LQG problem consists of two parts, the LQ control and a Kalman filter. The former in this case has been designed the way it was for the LQ control of the enlarged system reported in Section 2.2. As far as the Kalman Filter is concerned, there should be certain observability and reachability checks in LQG control problems. Therefore, one should make sure that the pair $(A, C_{q_{kf}}^T)$ is reachable, where $C_{q_{kf}} = \sqrt{Q_{kf}}$. Moreover, the pair (A, C_y) must be observable as

well. After some computations it turns out that the pair mentioned are fully ranked, thus satisfying the necessary conditions to solve the LQG problem. The dynamics equation of the Kalman filter then takes the following form:

$$\delta\dot{\hat{x}} = A\delta\hat{x} + B\delta u + \bar{L}_{kf}\left[\delta y - C_y\delta\hat{x}\right] = \left(A - \bar{L}_{kf}C_y\right)\delta\hat{x} + \begin{bmatrix} B & \bar{L}_{kf} \end{bmatrix}\begin{bmatrix} \delta u \\ \delta y \end{bmatrix}$$

The gain $\bar{L}_{kf}$ is obtained using the algebraic Riccati Equation and is as follows:

$$\bar{L}_{kf} = \begin{bmatrix} 3.1611 & 0.0046 \\ 0.0046 & 3.1535 \end{bmatrix}$$

After implementing the block diagram shown in Figure 2.21 in Simulink with the same experiment of load flow rate (w) as in the previous simulations, we end up with the following water temperature response:

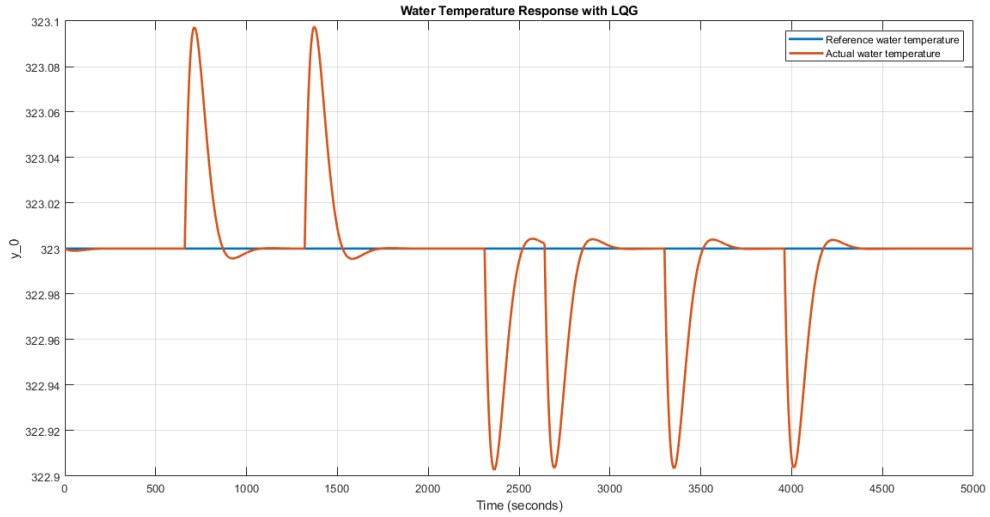

Figure 2.22: Water Temperature Response with LQG

As can be seen from Figure 2.22, the thermo-hydraulic plant does not show an oscillatory response, and the settling time here is around 600 time units, which is more or less the same as that of the LQ control in Section 2.2. In addition to that, the response is associated with peaks at 322.9027 and 323.0976, which is again negligible comparing to the reference value at $T^0 = 323$. Note that the goal of zero-error tracking is reached with LQG control too.

Speaking of LQG control, it is worth mentioning the estimated states too. In Figure 2.23 you can see that the state estimations are fulfilled successfully by the Kalman

Filter designed above. Note that the root mean square error between the first state and its estimate is 0.0017

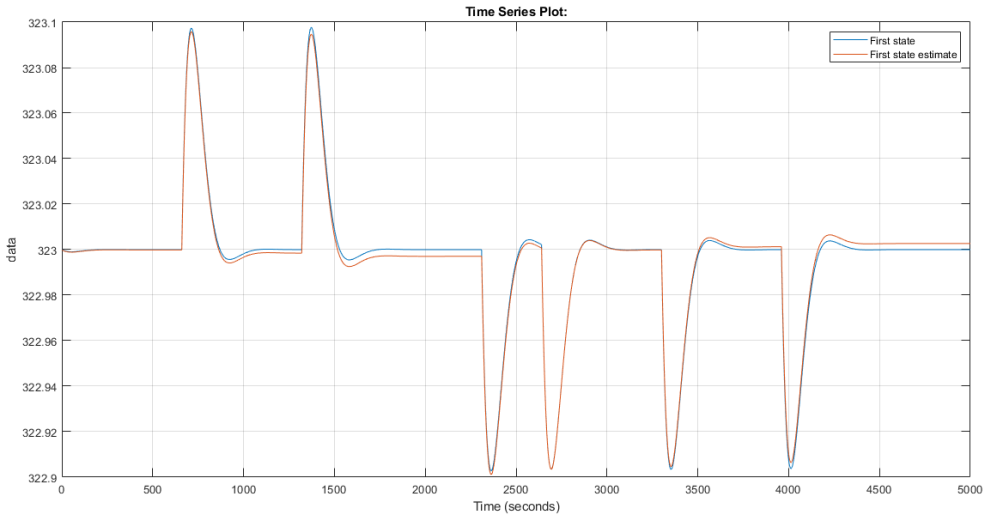

Figure 2.23: First state estimate with LQG

You can see the second state, which is at the same time the second output of the non-linear thermo-hydraulic plant, i.e., the metal temperature, along with its estimate by the Kalman filter below. The RMSE for this pair is 0.1098. Note that due the non-linearity of the system, metal temperature response is different at different operating points as was the case for the control methods described by now.

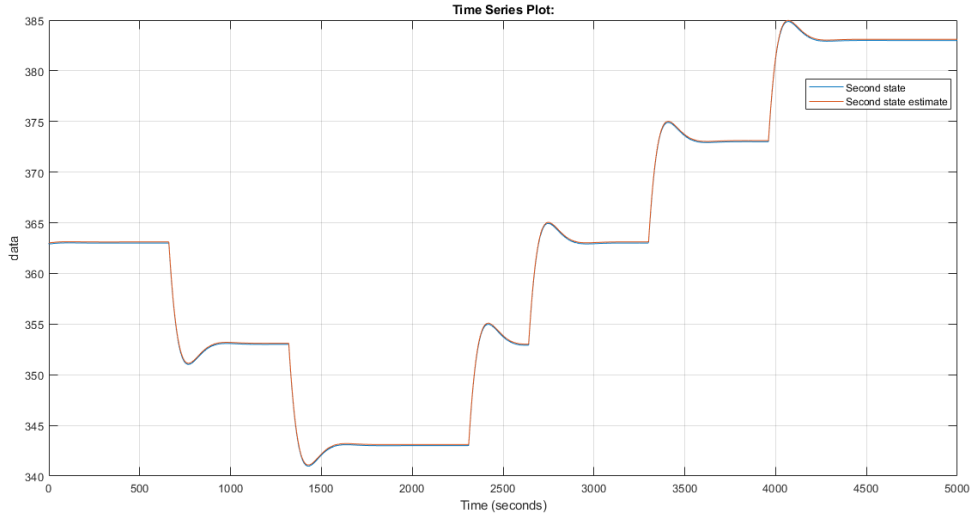

Figure 2.24: Second state estimate with LQG

2.5. H_2 and H_∞ control

In this chapter, we design a controller based on H_2 and H_∞ norms, and with shaping functions, for the thermo-hydraulic system. Before going into details, let us define some functions as shown below. Consider the SISO feedback system of Figure 2.25:

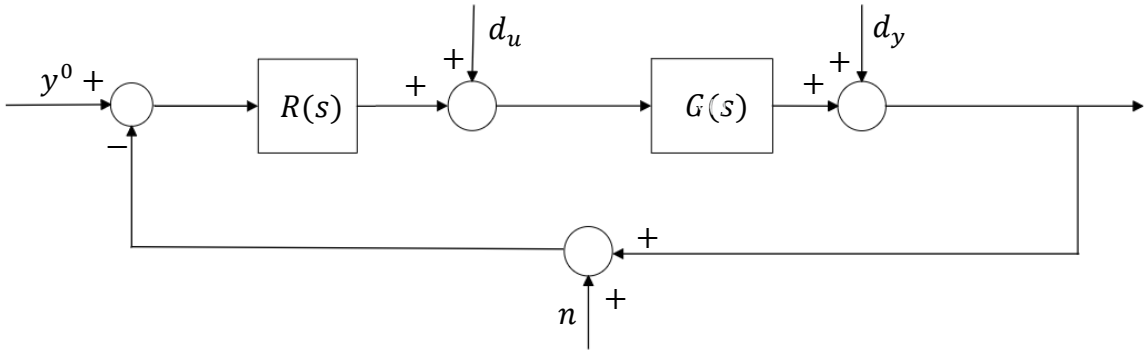

Figure 2.25: Control scheme

The loop contains exogenous and main signals, and the main relations between them are:

1. Loop transfer function:
$$L(s) = R(s)G(s)$$

2. Sensitivity:
$$S(s) = \frac{1}{1 + R(s)G(s)}$$

3. Complementary sensitivity:
$$T(s) = \frac{R(s)G(s)}{1 + R(s)G(s)} = 1 - S(s)$$

4. Control sensitivity:
$$K(s) = \frac{R(s)}{1 + R(s)G(s)} = S(s)R(s)$$

It also follows that

$$Y(s) = T(s)\big(Y^0(s) - N(s)\big) + S(s)D_y(s) + S(s)G(s)D_u(s)$$

$$U(s) = K(s)\big(Y^0(s) - N(s) - D_y(s)\big) + S(s)D_u(s)$$

To this end, it is usually advisable to design a controller based on the following criteria:

a. $|S|$ is small, thus $|L|$ is big, at usually low frequencies where the system disturbance's spectrum (d_y) contains significant harmonic components
b. $|T|$ is roughly equal to one, thus $|L|$ is big at usually low to medium frequencies where the system reference signal's spectrum (y^0) contains significant harmonic components
c. $|T|$ is small, thus $|L|$ is small at usually high frequencies where the measurement noise spectrum (n) contains significant harmonic components

Moreover, it is worth mentioning that when the loop transfer function $L(s)$ has one or more integrators, its modulus is high at low frequencies, which guarantees asymptotic zero error tracking given constant disturbances d_y and a constant reference signal y^0.

Let us recall that the peaks of the sensitivity function and the complementary sensitivity function are defined as follows:

$$M_S = \sup_{\omega} S(j\omega) = \|S\|_\infty$$

$$M_T = \sup_{\omega} T(j\omega) = \|T\|_\infty$$

The minimum distance from the -1 point of the Nyquist diagram of $L(j\omega)$ is M_S^{-1}. Furthermore, considering that the sum of the two functions hold the following relation:

$$S(s) + T(s) = 1$$

It is also true that

$$\big||S(j\omega)| + |T(j\omega)|\big| \leq |S(j\omega) + T(j\omega)| = 1, \quad \forall\omega$$

In the controller design, it is advised to meet the following requirements based on the above-given considerations:

$$M_S \leq \bar{M}_S$$

$$M_T \leq \bar{M}_T$$

where usually $\bar{M}_S = 2\ (6dB)$ and $\bar{M}_T = 1.5\ (2dB)$.

As already mentioned, the sensitivity and complementary sensitivity functions are widely used in design specifications. Let us assume that $|S(j\omega)|$ crosses -3dB at ω_B from below, and $|T(j\omega)|$ crosses -3dB at ω_B from above at ω_{BT}. We then can conclude that $\omega_B < \omega_c < \omega_{BT}$, for a phase margin less than 90° ($\varphi_m < 90°$). Now one can have the following design specifications on the sensitivity function:

- A minimum frequency ω_B
- A zero or small asymptotic error given a constant reference signal
- A suitable shape of $|S(j\omega)|$
- $M_S \leq \bar{M}_S$

These four specifications can be formally rewritten in the form stated below:

$$|S(j\omega)| < \frac{1}{|W_S(j\omega)|}, \quad \forall\omega$$

Here $W_S(j\omega)$ is called the sensitivity shaping function that is supposed be defined by the designer. As can be observed, this shaping function is an inverse of an ideal sensitivity function. This requirement can be formulated using an H_∞ norm as reported below:

$$\|W_S S\|_\infty < 1$$

where the shaping function can be chosen as

$$W_S(s) = \frac{\frac{s}{M} + \omega_B}{s + A\omega_B}$$

Note that M is the desired bound of the H_∞ norm of $S(s)$ and $A \ll 1$ is a desired attenuation in the required band of interest.

Similarly, a possible choice of another shaping function $W_T(s)$ can be made based on $T(s)$. In addition, a proper selection of A and M can be done according to the previous considerations.

$$|T(j\omega)| < \frac{1}{|W_T(j\omega)|}, \quad \forall\omega \leftrightarrow \|W_T T\|_\infty < 1$$

$$W_T(s) = \frac{s + \frac{\omega_{BT}}{M}}{As + \omega_{BT}}$$

The control variable, as it has been reported above, is defined by

$$U(s) = K(s)Y^0(s)$$

In the design process of a controller based on shaping functions, one must set

$$|K(j\omega)| < \frac{1}{|W_K(j\omega)|}, \qquad \forall\omega \leftrightarrow \|W_K K\|_\infty < 1$$

Note that the shaping function $W_S(s)$, $W_T(s)$, $W_K(s)$ are used in open loop, thus they should be asymptotically stable systems.

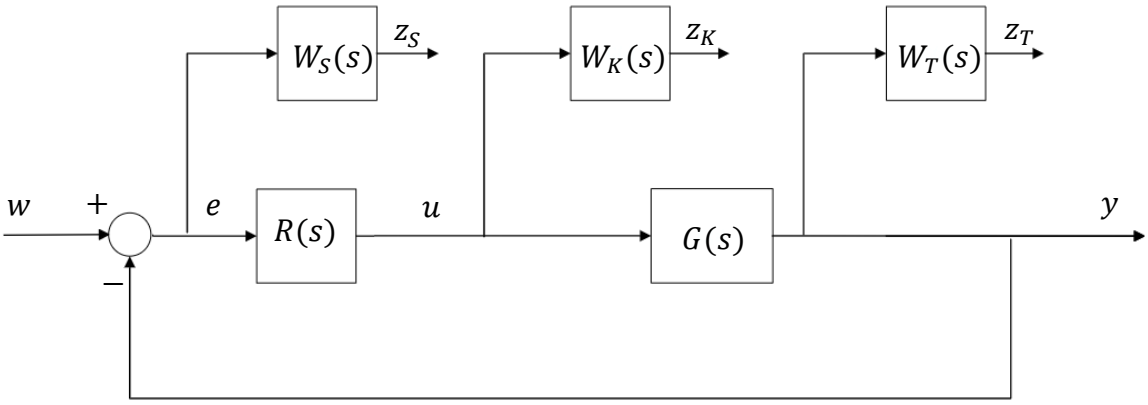

Figure 2.26: Control system with the shaping functions

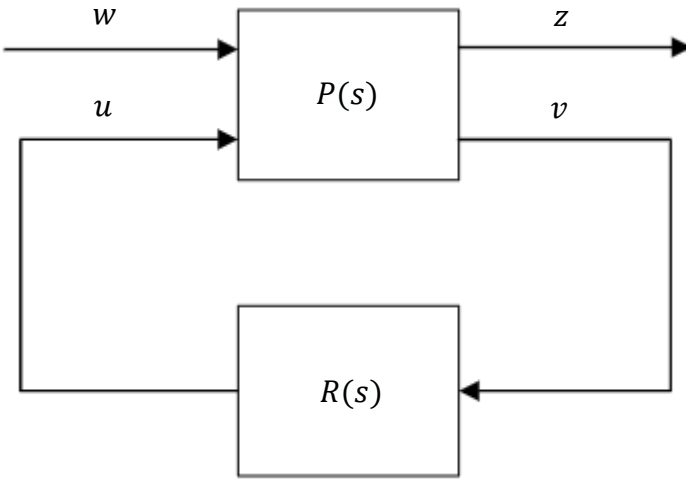

Figure 2.27: Control scheme for H_2 and H_∞ control

In accordance with Figure 2.26, define the following:

$$z = \begin{bmatrix} z_S \\ z_K \\ z_T \end{bmatrix}, \quad w = y^0$$

Note that z corresponds to the performance variables, while w is the exogenous signal. Let us define $G_{zw}(s)$ as follows, which is the transfer function from w to z when the plant $G(s)$ is enlarged with the aforementioned shaping functions and the resulted enlarged system is fed back through the regulator $R(s)$:

$$G_{zw}(s) = \begin{bmatrix} W_S(s)S(s) \\ W_T(s)T(s) \\ W_K(s)K(s) \end{bmatrix}$$

Then the regulator can be synthesized by minimizing $G_{zw}(j\omega)$. This method of regulator synthesis is, thus, called the H_∞ control:

$$\|G_{zw}\|_\infty = \sup_\omega \bar{\sigma}(G_{zw}(j\omega))$$

If the regulator follows the relation $\|G_{zw}\|_\infty < \gamma$, we also have

$$\|W_S S\|_\infty < \gamma, \quad \|W_T T\|_\infty < \gamma, \quad \|W_K K\|_\infty < \gamma,$$

A slightly different synthesis approach is the H_2 control and it requires the minimization of

$$J = \frac{1}{2\pi}\int_{-\infty}^{+\infty} (|W_S(j\omega)S(j\omega)|^2 + |W_T(j\omega)T(j\omega)|^2 + |W_K(j\omega)K(j\omega)|^2)d\omega$$
$$= \frac{1}{2\pi}\int_{-\infty}^{+\infty} (|G_{zw}(j\omega)|^2)d\omega$$

The point of the H_2 and H_∞ control problems is to minimize the corresponding norm of the transfer function G_{zw} in the enlarged system $P(s)$ reported in Figure 2.27 with respect to the regulator $R(s)$. $P(s)$ can be represented by a general state-space form from which a matrix P can be driven as shown below:

$$\dot{x}(t) = Ax(t) + B_1 w(t) + B_2 u(t)$$
$$z(t) = C_1 x(t) + D_{11} w(t) + D_{12} u(t)$$
$$v(t) = C_2 x(t) + D_{21} w(t) + D_{22} u(t)$$
$$P = \begin{bmatrix} A & B_1 & B_2 \\ C_1 & D_{11} & D_{12} \\ C_2 & D_{21} & D_{22} \end{bmatrix}$$

where the matrices B_1, B_2, C_1, C_2, D_{11}, D_{12}, D_{21}, D_{22} are to be selected based on the design requirements.

In order to design an H_2 and H_∞ controller with shaping functions, consider again the scheme reported in Figure 2.26. Consider the alternative block diagram of such system below:

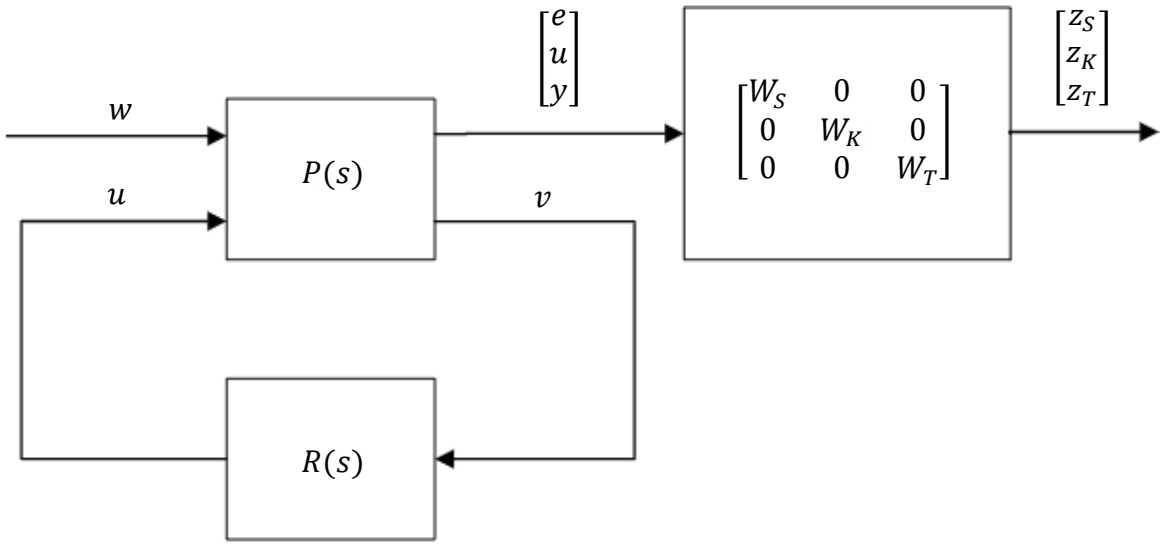

Figure 2.28: Equivalent scheme for shaping function at the process output

Note that the following representation, based on Figure 2.28, holds:

$$Z_S(s) = W_S(s)S(s)W(s), \quad Z_T(s) = W_T(s)T(s)W(s), \quad Z_K = W_K(s)R(s)S(s)W(s)$$

Letting the shaping functions be described as follows:

$W_S(s)$:

$$\dot{x}_S(t) = A_S x_S(t) + B_S(w(t) - y(t))$$
$$z_S(t) = C_S x_S(t)$$

$W_K(s)$:

$$\dot{x}_K(t) = A_K x_K(t) + B_K u(t)$$
$$z_K(t) = C_K x_K(t) + D_K u(t)$$

$W_T(s)$:

$$\dot{x}_T(t) = A_T x_T(t) + B_T y(t)$$
$$z_T(t) = C_T x_T(t) + D_T y(t)$$

Finally, the compact form for the enlarged system with shaping functions at the output becomes

$$\begin{bmatrix} \dot{x}(t) \\ \dot{x}_S(t) \\ \dot{x}_K(t) \\ \dot{x}_T(t) \end{bmatrix} = \begin{bmatrix} A & 0 & 0 & 0 \\ -B_S C & A_S & 0 & 0 \\ 0 & 0 & A_K & 0 \\ B_T C & 0 & 0 & A_T \end{bmatrix} \begin{bmatrix} x(t) \\ x_S(t) \\ x_K(t) \\ x_T(t) \end{bmatrix} + \begin{bmatrix} B \\ 0 \\ B_K \\ 0 \end{bmatrix} u(t) + \begin{bmatrix} 0 \\ B_S \\ 0 \\ 0 \end{bmatrix} w(t)$$

$$\begin{bmatrix} z_S(t) \\ z_K(t) \\ z_T(t) \end{bmatrix} = \begin{bmatrix} 0 & C_S & 0 & 0 \\ 0 & 0 & C_K & 0 \\ D_T C & 0 & 0 & C_T \end{bmatrix} \begin{bmatrix} x(t) \\ x_S(t) \\ x_K(t) \\ x_T(t) \end{bmatrix} + \begin{bmatrix} 0 \\ D_K \\ 0 \end{bmatrix} u(t) + \begin{bmatrix} 0 \\ 0 \\ 0 \end{bmatrix} w(t)$$

$$v(t) = \begin{bmatrix} -C & 0 & 0 & 0 \end{bmatrix} \begin{bmatrix} x(t) \\ x_S(t) \\ x_K(t) \\ x_T(t) \end{bmatrix} + w(t)$$

Let us design an H_2 controller based on this. We initially define sensitivity functions. Note that $W_S(s)$ is an inverse of a desired sensitivity function. For this, recall the form of the sensitivity shaping function as already mentioned earlier:

$$W_S(s) = \frac{\frac{s}{M} + \omega_B}{s + A\omega_B}$$

Based on this consideration, we have

1. $\omega_B = 10$, the desired bandwidth. We treat this variable carefully since by changing it we might completely change the system design requirements. For example, when we increase the bandwidth from 10 to 100, the system becomes 10 times faster.
2. $A = 10^{-8}$, the desired disturbance attenuation inside the bandwidth. Notice that we want the sensitivity function to be around $-160\,dB$ at lower frequencies up to the bandwidth ω_B. By assigning A to this value, the reverse will be true, i.e., $W_s(s)$ will be $160\,dB$ at low frequencies.
3. $M = 2$, the desired bound on $\|S\|_\infty$ and $\|T\|_\infty$. This value corresponds to the peak value for the ideal sensitivity function, that is $W_s(s)$ will remain at the lowest value of $2\,dB$ at high frequencies.

The same applies for $W_T(s)$ assuming that it is an inverse of the ideal complementary sensitivity function. Note also that the choices should be coherent, so that the sum of the sensitivity and complementary sensitivity functions should be identity. Therefore, $\omega_B = \omega_{BT} = 10$. Here are the sensitivity, complementary sensitivity and control sensitivity functions along with their Bode diagrams:

$$W_S(s) = \frac{s+2}{2s+0.0002}, \quad W_K(s) = \frac{0.001s+1}{0.01s+1}, \quad W_T(s) = \frac{s+0.5}{0.0001s+1}$$

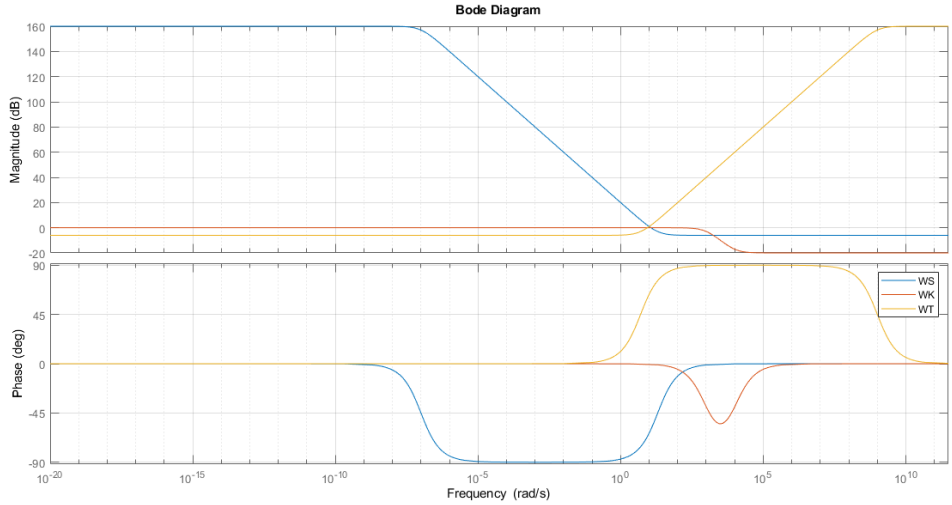

Figure 2.29: Bode plots of the shaping functions

After augmenting the system with ***augw*** command of MATLAB, we synthesize the H_2 and H_∞ controllers:

$$R_{H_2 shape}(s) = \frac{198.3s^4 + 1.983 \cdot 10^{11}s^3 + 1.983 \cdot 10^{14}s^2 + 3 \cdot 10^{12}s + 1.16 \cdot 10^{10}}{s^5 + 10^9 s^4 + 10^{13}s^3 + 6.025 \cdot 10^{12}s^2 + 1.814 \cdot 10^{12}s + 6.652 \cdot 10^7}$$

$$R_{H_\infty shape}(s) = \frac{102.9s^4 + 1.03 \cdot 10^{11}s^3 + 1.03 \cdot 10^{14}s^2 + 1.314 \cdot 10^{12}s + 3.641 \cdot 10^9}{s^5 + 10^9 s^4 + 10^{13}s^3 + 4.821 \cdot 10^{12}s^2 + 1.168 \cdot 10^{12}s + 3.719 \cdot 10^5}$$

In the diagrams below, the loop transfer functions corresponding to the H_2 and H_∞ controllers are given for comparison reasons. Compared to the standard LQG control problem whose performance was not satisfactory enough, both controllers allow the loop transfer function to be 0 dB at low frequencies and to have a proper attenuation at higher frequencies, which is desired.

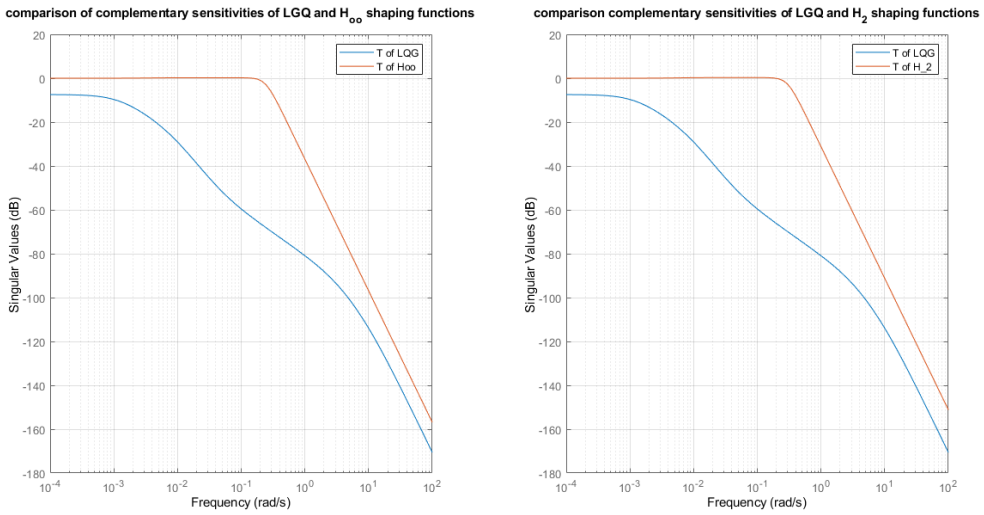

Figure 2.30: Comparison on loop transfer functions of LQG versus H_∞ and H_2

Implementing the controller $R_{H_2 shape}(s)$ and $R_{H_\infty shape}(s)$ in the thermo-hydraulic plant, we get the following water temperature responses:

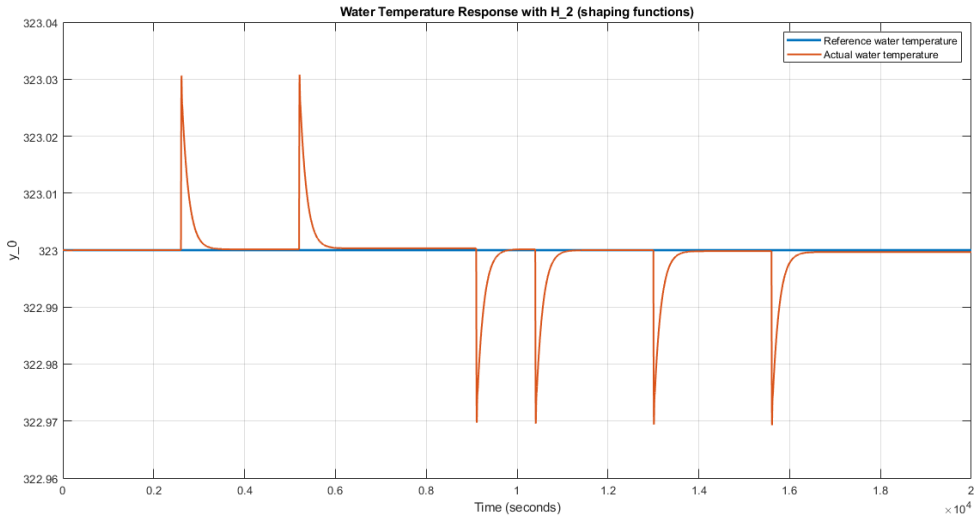

Figure 2.31: Water temperature response with H_2 using shaping functions

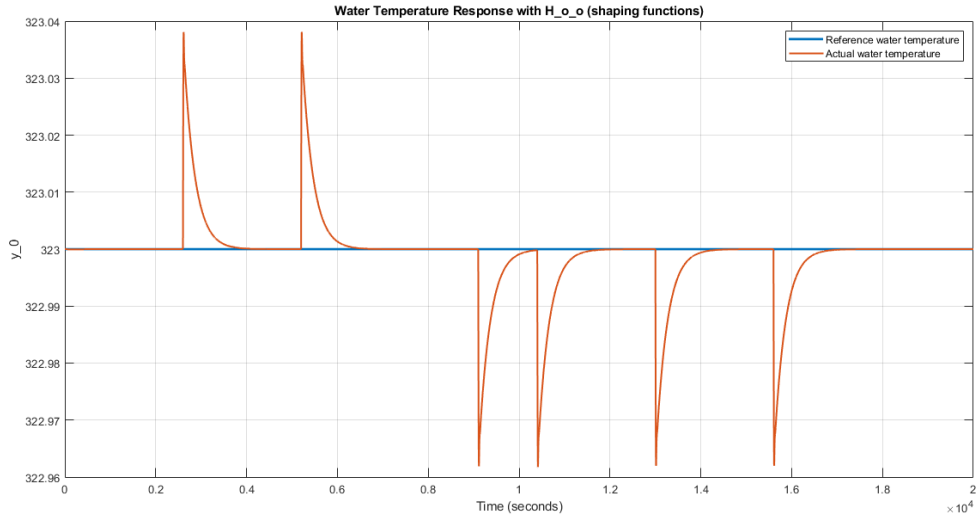

Figure 2.32: Water temperature response with H_∞ using shaping functions

As can be seen from the water temperature responses, both of the controllers are able to provide zero error tracking with the H_∞ controller being slightly better. Moreover, the deviation from the reference value of the water temperature $T^0 = 323$ is negligibly small, varying in the range [322.9693, 323.0308] and [322.9618, 323.0381] for H_2 and H_∞ controllers, respectively. The settling time for these responses is equal to more or less 100 times units. In general, it can be concluded that the control structure designed using the shaping functions specified above does provide stability around the reference value. Furthermore, the system behaves well at operating points far from the nominal operating condition where the original controllers were constructed.

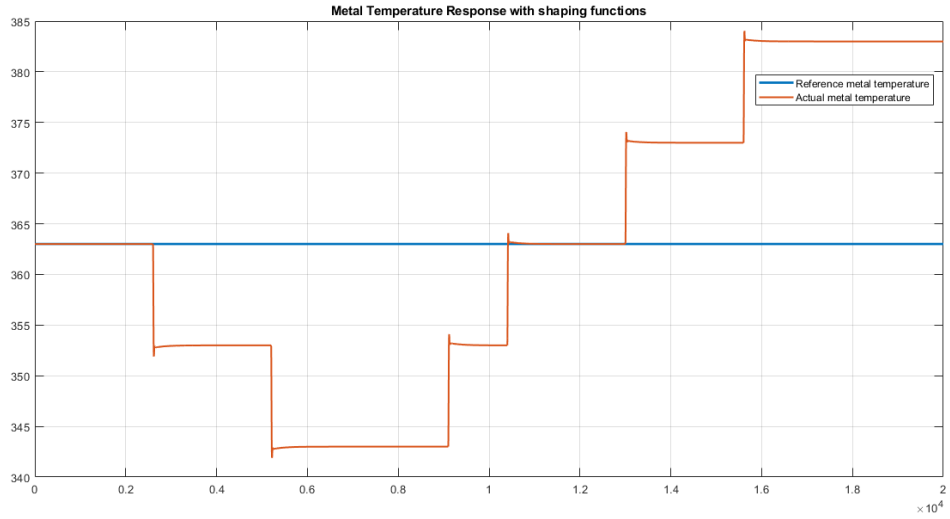

Figure 2.33: Metal temperature response with shaping functions

Figure 2.33 shows the metal temperature response of the thermo-hydraulic system. It is obvious in the presence of the varying load flow rate w, the step response is quite different at different operating points, which is obvious in view of the nonlinearity of the system.

2.6. Backstepping control

In the control literature, there can be found a huge diversity of techniques applied to non-linear systems, one of which is backstepping. In this paragraph, aiming to achieve disturbance rejection, we implement this recursive method also known as an integrator backstepping. Consider the following system:

$$\dot{x}_1(t) = f\big(x_1(t)\big) + g\big(x_1(t)\big)x_2(t) \quad , \quad x_1 \in R^n, \qquad x_2 \in R^1$$

$$\dot{x}_2(t) = u(t)$$

Here f and g are differentiable and continuous functions in a set $D \subset R^n$ and $f(0) = 0$. Assuming that x_2 is a virtual design variable, so that to stabilize the first equation of the aforementioned set using a control law. We omit the time dependence for convenient notation.

$$x_2 = \phi_1(x_1), \qquad \phi_1(0) = 0$$

Therefore, the closed loop system takes the form

$$\dot{x}_1 = f(x_1) + g(x_1)\phi_1(x_1)$$

Choose a Lyapunov function such that

$$\dot{V}_1(x_1) = \frac{dV_1}{dx_1}\big(f(x_1) + g(x_1)\phi_1(x_1)\big) = -W(x_1), \quad W(x_1) \geq 0, x_1 \in D$$

Recalling that the state variable cannot be arbitrarily chosen, we define the error term

$$\eta = x_2 - \phi_1(x_1)$$

The derivative of the error term thus takes the following form:

$$\begin{aligned}\dot{\eta} &= \dot{x}_2 - \dot{\phi}_1(x_1) = u - \frac{\phi_1(x_1)}{dx_1}\dot{x}_1 \\ &= u - \frac{d\phi_1(x_1)}{dx_1}[f(x_1) + g(x_1)(\eta + \phi_1(x_1))]\end{aligned}$$

As a result, the original system can be rewritten as:

$$\dot{x}_1 = f(x_1) + g(x_1)(\eta + \phi_1(x_1))$$

$$\dot{\eta} = u - \frac{\phi_1(x_1)}{dx_1}[f(x_1) + g(x_1)(\eta + \phi_1(x_1))]$$

Define a new input v

$$v = u - \dot{\phi}_1(x_1)$$

Also recall $\dot{\eta} = v$. Therefore, the system can be represented as

$$\dot{x}_1 = f(x_1) + g(x_1)\phi_1(x_1) + g(x_1)\eta$$

$$\dot{\eta} = v$$

In this equations, one can conclude that the equilibrium of the first subsystem at the origin is asymptotically stable. For this, we can choose a Lyapunov function for the overall system:

$$V_2(x_1, \eta) = V_1(x_1) + \frac{1}{2}\eta^2 = V_1(x_1) + \frac{1}{2}\big(x_2 - \phi_1(x_1)\big)^2$$

$$\dot{V}_2(x_1,\eta) = \frac{dV_1(x_1)}{dx_1}\dot{x}_1 + \eta\dot{\eta}$$
$$= \frac{dV_1(x_1)}{dx_1}(f(x_1) + g(x_1)\phi_1(x_1) + g(x_1)\eta) + \eta v$$
$$\leq -W(x_1) + \frac{dV_1(x_1)}{dx_1}g(x_1)\eta + \eta v$$

By setting the following relation

$$v = -\frac{dV_1(x_1)}{dx_1}g(x_1) - k\eta, \quad k > 0$$

we obtain

$$\dot{V}_2(x_1,\eta) = -W(x_1) - k\eta^2 < 0$$

Thus, the equilibrium $(x_1 = 0, \eta = 0)$ is asymptotically stable. Based on the considerations, it turns out that the original equilibrium $(x_1 = 0, x_2 = 0)$ is asymptotically stable too, since $\eta = x_2 - \phi_1(x_1)$ and $\phi_1(0) = 0$.

The final control for the overall system becomes

$$u = v + \dot{\phi}_1(x_1) = -\frac{dV_1(x_1)}{dx_1}g(x_1) - k\eta + \dot{\phi}_1(x_1) =$$
$$= -\frac{dV_1(x_1)}{dx_1}g(x_1) - k\big(x_2 - \phi_1(x_1)\big) + \frac{d\phi_1(x_1)}{dx_1}(f(x_1)$$
$$+ g(x_1)x_2)$$

Also note that with the following Lyapunov function we can show that the asymptotic stability is guaranteed at the origin:

$$V_2(x_1,x_2) = V_1(x_1) + \frac{1}{2}\eta^2 = V_1(x_1) + \frac{1}{2}\big(x_2 - \phi_1(x_1)\big)^2$$

To generalize this notion, let us consider the following system

$$\dot{x}_1(t) = f_1\big(x_1(t)\big) + g_1\big(x_1(t)\big)x_2(t) \quad , \quad x_1 \in R^n, x_2 \in R^1$$
$$\dot{x}_2(t) = f_2\big(x_1(t), x_2(t)\big) + g_2(x_1(t), x_2(t))u(t)$$

We again assume the functions f_2 and g_2 to be differentiable and continuous and $g_2(x_1, x_2) \neq 0$. Then we can set the following by considering a fictitious input:

$$u = \frac{1}{g_2(x_1,x_2)}(u_a - f_2(x_1,x_2))$$

Therefore, the system equation can be rewritten as

$$\dot{x}_1 = f_1(x_1) + g_1(x_1)x_2$$

$$\dot{x}_2 = u_a$$

Based on the previously given considerations, we can conclude that the control law is

$$u = \frac{1}{g_2(x_1, x_2)}\left\{\frac{d\phi_1(x_1)}{dx_1}\,(f_1(x_1) + g_1(x_1)x_2) - k\big(x_2 - \phi_1(x_1)\big) - \frac{dV_1(x_1)}{dx_1}\,g_1(x_1) - f_2(x_1, x_2)\right\}$$

given that $x_2 = \phi(x_1)$ stabilizes the first subsystem's equilibrium at the origin with the corresponding Lyapunov function $V_1(x_1)$.

The Lyapunov function corresponding to the feedback system can be selected as follows:

$$V_2(x_1, x_2) = V_1(x_1) + \frac{1}{2}\big(x_2 - \phi_1(x_1)\big)^2$$

Recall that in the thermo-hydraulic system, the control variable is the gas flow rate w_c, whereas its manipulated variable is the water temperature T. Consider the state equations below:

$$\begin{cases} \dfrac{dT}{dt} = \dfrac{1}{\rho A z}\left[w(T_i - T) + \dfrac{k_{lm}A}{c}(T_m - T)\right] \\ \dfrac{dT_m}{dt} = \dfrac{1}{M_m c_m}\left[-k_{lm}A(T_m - T) + \sigma k_f w_c (T_f^4 - T_m^4)\right] \end{cases}$$

Note that both of the states of the system are available and $[x_1\ x_2]^T = [T\ \ T_m]^T$. For convenience, with minor changes, the system is transformed into the following equivalent form given below:

$$\dot{x}_1 = \varphi_1 - \varphi_2 x_1 + \varphi_3(x_2 - x_1)$$

$$\dot{x}_2 = \varphi_4(x_2 - x_1) + \varphi_6(\varphi_5 - x_2^4)w_c$$

where

$$\varphi_1 = \frac{wT_i}{\rho A z},\quad \varphi_2 = \frac{w}{\rho A z},\quad \varphi_3 = \frac{k_{lm}A}{c\rho A z}$$

$$\varphi_4 = -\frac{k_{lm}A}{M_m c_m}, \quad \varphi_5 = T_f^4 \quad \varphi_6 = \frac{\sigma k_f}{M_m c_m}$$

Note that the equilibrium points for the states of the system are not the origin, i.e., $[\bar{T} \quad \bar{T}_m]^T = [\bar{x}_1 \quad \bar{x}_2] = [323 \quad 363]^T$. Moreover, the equilibrium point of the control variable is at 0.112. Therefore, the backstepping algorithm requires a modified definition of state variables, as shown below:

$$\begin{cases} z_1 \triangleq x_1 - \bar{x}_1 = x_1 - 323 \\ z_2 \triangleq x_2 - \bar{x}_2 = x_2 - 363 \\ w_c \triangleq u - \bar{u} = u - 0.112 \end{cases} \Leftrightarrow \begin{cases} x_1 = z_1 + 323 \\ x_2 = z_2 + 363 \\ w_c = u + 0.112 \end{cases}$$

Thus, we should substitute the expressions reported above in the original state equations:

$$\frac{d}{dt}(z_1 + 323) = \varphi_1 - \varphi_2(z_1 + 323) + \varphi_3((z_2 + 363)) - (z_1 + 323))$$

$$\frac{d}{dt}(z_2 + 363) = \varphi_4((z_2 + 363) - (z_1 + 323)) + \varphi_6(\varphi_5 - (z_2 + 363)^4)(u + 0.112)$$

By doing so, we have found and applied a change of state and control variables that translate the equilibrium of the thermo-hydraulic system to the origin. The equivalent system thus becomes:

$$\dot{z}_1 = \varphi_1 - 323\varphi_2 + 40\varphi_3 - z_1(\varphi_2 + \varphi_3) + \varphi_3 z_2$$

$$\dot{z}_2 = \varphi_4(z_2 - z_1 + 40) + 0.112\varphi_6(\varphi_5 - (z_2 + 363)^4) + \varphi_6(\varphi_5 - (z_2 + 363)^4)u$$

We now design a backstepping controller for this system. Note that the following relations hold for the system under control:

$$\dot{z}_1 = f_1(z_1) + g_1(z_1)z_2$$

$$\dot{z}_2 = f_2(z_1, z_2) + g_2(z_1, z_2)u$$

where

$$f_1(z_1) = \varphi_1 - 323\varphi_2 + 40\varphi_3 - z_1(\varphi_2 + \varphi_3)$$

$$g_1(z_1) = \varphi_3$$

$$f_2(z_1, z_2) = \varphi_4(z_2 - z_1 + 40) + 0.112\varphi_6(\varphi_5 - (z_2 + 363)^4)$$

$$g_2(z_1, z_2) = \varphi_6(\varphi_5 - (z_2 + 363)^4)$$

We can switch to the basic backstepping canonical form for convenience by introducing an arbitrary control input u_a. The relation between the overall control law and u_a is as follows:

$$u = \frac{1}{g_2(z_1, z_2)}[u_a - f_2(z_1, z_2)]$$

Then it follows

$$\dot{z}_1 = f_1(z_1) + g_1(z_1)z_2$$

$$\dot{z}_2 = u_a$$

Now assume $z_2 = \phi_1(z_1)$, which will later be used to find u_a. Let us define

$$\phi_1(z_1) = \frac{-\varphi_1 + 323\varphi_2 - 40\varphi_3 - z_1}{\varphi_3}$$

Thus

$$\begin{aligned}\dot{z}_1 = f_1(z_1) + g_1(z_1)\left(\frac{-\varphi_1 + 323\varphi_2 - 40\varphi_3 - z_1}{\varphi_3}\right) \\ = \varphi_1 - 323\varphi_2 + 40\varphi_3 - z_1(\varphi_2 + \varphi_3) - \varphi_1 + 323\varphi_2 - 40\varphi_3 \\ - z_1 = -z_1(\varphi_2 + \varphi_3 + 1)\end{aligned}$$

Now we need to choose a Lyapunov function that is radially unbounded, continuous with its derivatives and positive definite depending on only z_1:

$$V_1(z_1) = \frac{1}{2}x_1^2$$

Therefore,

$$\dot{V}_1(z_1) = z_1\dot{z}_1 = z_1\big(-z_1(\varphi_2 + \varphi_3 + 1)\big) = -(\varphi_2 + \varphi_3 + 1)z_1^2$$

Since $(\varphi_2 + \varphi_3 + 1) > 0$ for every value of the load disturbance, the derivative of the Lyapunov function is negative definite, that is $\dot{V}_1(z_1) < 0$. Therefore, we can proceed to determine u_a, which will in turn lead to the final control law u, or we can directly use the extended formula as shown below:

$$\begin{aligned}u = \frac{1}{g_2(z_1, z_2)}\left\{\frac{d\phi_1(z_1)}{dz_1}\,(f_1(z_1) + g_1(z_1)z_2) - k\big(z_2 - \phi_1(z_1)\big)\right. \\ \left. - \frac{dV_1(z_1)}{dz_1}g_1(z_1) - f_2(z_1, z_2)\right\}\end{aligned}$$

$$u = \frac{1}{g_2(z_1, z_2)}\left\{-(f_1(z_1) + g_1(z_1)z_2) - k\left(z_2 - \frac{-\varphi_1 + 323\varphi_2 - 40\varphi_3}{\varphi_3}\right) - \varphi_3 z_1 - f_2(z_1, z_2)\right\}$$

where $f_1(z_1)$, $g_1(z_1)$, $f_2(z_1, z_2)$ and $g_2(z_1, z_2)$ are given as already shown earlier:

$$f_1(z_1) = \varphi_1 - 323\varphi_2 + 40\varphi_3 - z_1(\varphi_2 + \varphi_3)$$

$$g_1(z_1) = \varphi_3$$

$$f_2(z_1, z_2) = \varphi_4(z_2 - z_1 + 40) + 0.112\varphi_6(\varphi_5 - (z_2 + 363)^4)$$

$$g_2(z_1, z_2) = \varphi_6(\varphi_5 - (z_2 + 363)^4)$$

Here k is a tuning parameter to be suitably selected. Initially, $k = 0.009$, so that there is no need for a saturation block in Simulink. To this end, the control input will take reasonable values during simulations, typically not exceeding the range that we have achieved with other controllers above.

To check the global asymptotic stability, we can use the Lyapunov function $V_2(z_1, z_2)$ below:

$$V_2(z_1, z_2) = V_1(z_1) + \frac{1}{2}\left(z_2 - \phi_1(z_1)\right)^2$$

Since $\dot{V}_2(z_1, z_2) < 0$, we deduce that the origin is globally asymptotically stable.

Let us have a look at how the thermo-hydraulic system's output T responds using this backstepping controller that we have just designed.

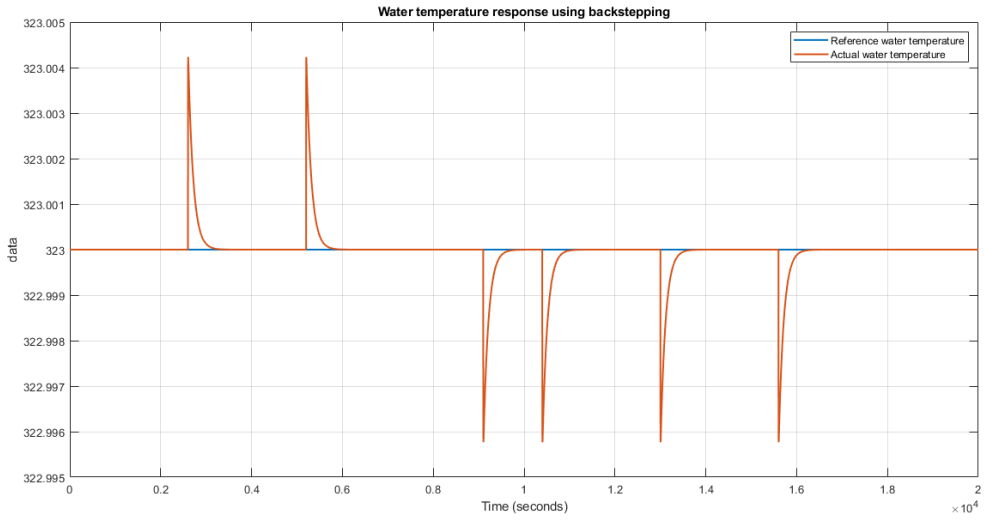

Figure 2.34: Water temperature response using backstepping

As can be seen from Figure 2.34, the water temperature converges to the equilibrium at $T = 323°$, in other words, the water temperature response reported shows that the backstepping controller is able to provide zero error tracking when disturbances are present in the system. Additionally, the settling time seems to be satisfactory at almost 200 time units. We clearly see that the backstepping control ensures global asymptotic stability. However, there are a few drawbacks that should be mentioned. Tuning the parameter k can sometimes be time-consuming. Theory holds if there is no saturation on the input variable u. Furthermore, the backstepping control technique requires an exact model of the plant along with its state measurements.

As it was seen in the previous controllers in this chapter, in the presence of the varying load flow rate w, the step response of the metal temperature is quite different at different operating points, which is obvious in view of the nonlinearity of the system, see Figure 2.35.

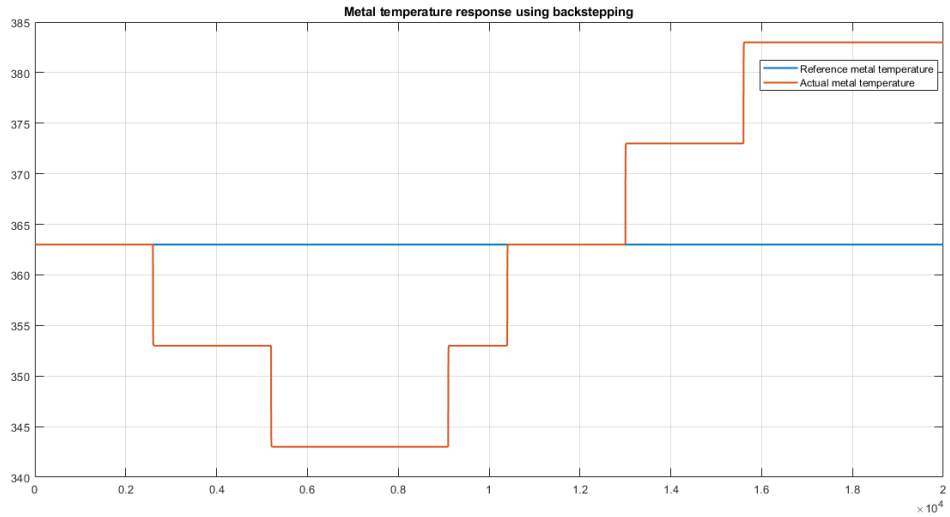

Figure 2.35: Metal temperature response using backstepping

3 Comparative study of controllers

In this chapter, the step response of the reference value of the water temperature of the nonlinear thermo-hydraulic plant by different control strategies mentioned in Section 2 will be compared to find out which works best for a given setpoint change. Additionally, their corresponding control actions will be considered too. Note that for a reference signal we use a step input that changes from 323° to 315° at the time instant of 1000. Special attention will be drawn to the control actions at that time instant, since at the steady-state the value of the control variable (the gas flow rate) is the same for all the controllers.

3.1. PI controller

The step output of the water temperature of the plant by the PI controller and the associated control signal are shown in Figure 3.1 and Figure 3.2, respectively.

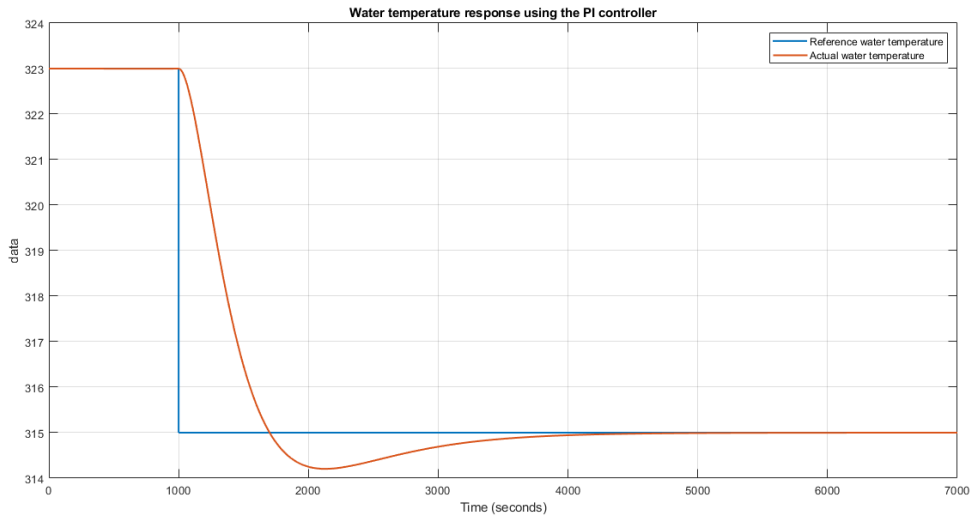

Figure 3.1: Step output for the PI controller

When one observes the actual water temperature response by the PI controller, it is clear that after some settling time of 3200 time instants the response is able to reach the desired water temperature at 315°. The risetime for the response is 476 time units, whereas the overshoot value is at 314.205.

As far as the control action is concerned, it has the fall to -0.04 at the time instant of 1000 where the step change happens.

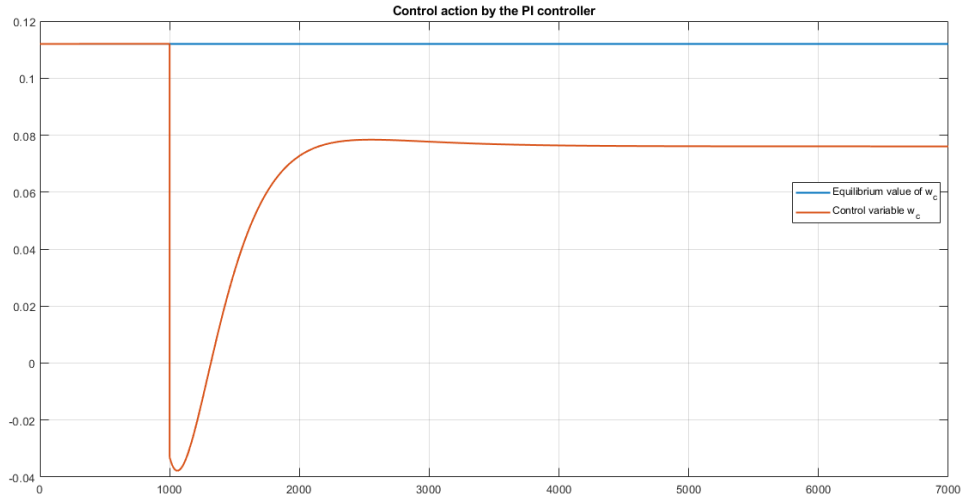

Figure 3.2: Control signal for the PI controller

3.2. Pole-placement controller

The step response of the water temperature of the plant by the pole-placement controller and the associated control signal are reported in figures below:

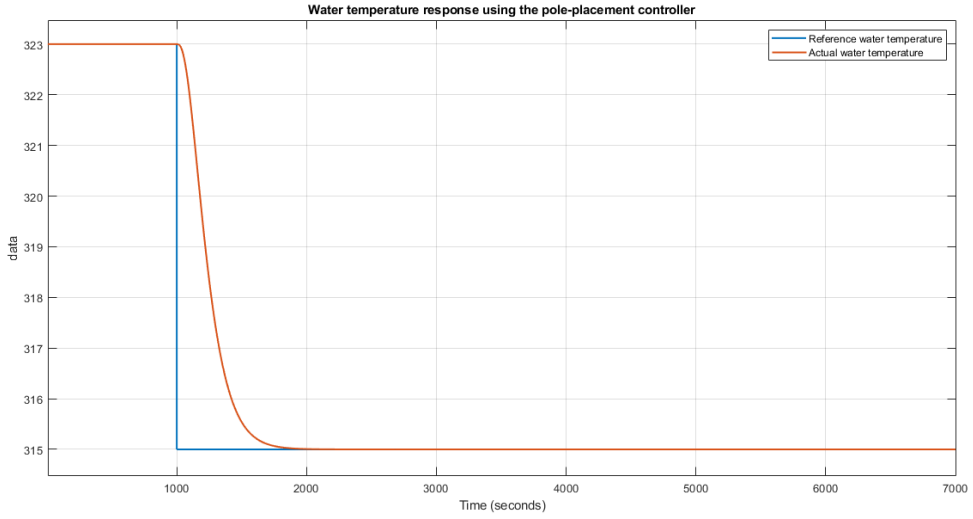

Figure 3.3: Step output for the pole-placement controller

Having a look at the actual water temperature response by the pole-placement controller, it becomes obvious that after some settling time of 1200 time instants the response is able to reach the desired water temperature at 315°. The risetime in this particular control strategy corresponds to 112 time instants, while the response does not show any overshoots.

However, the control action shows the fall to -0.18 at the time instant of 1000 where the step change happens.

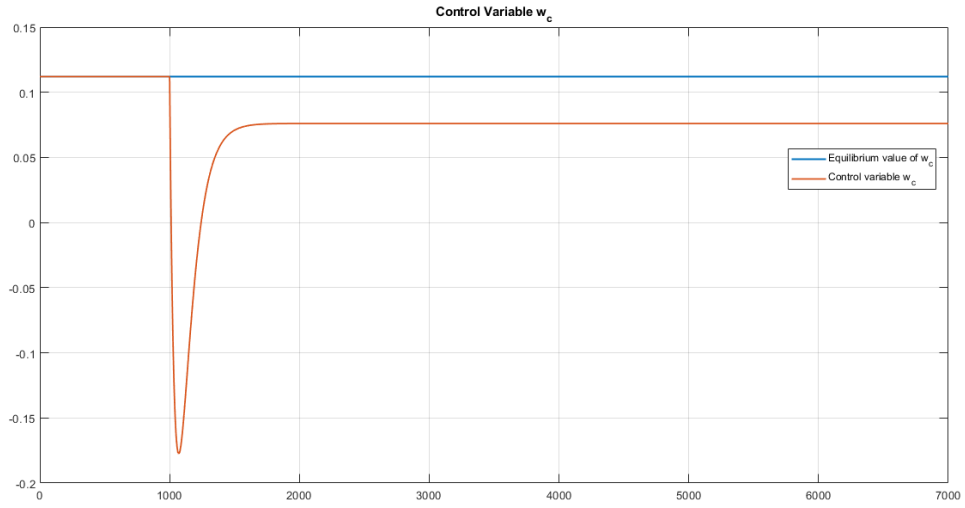

Figure 3.4: Control signal for the pole-placement controller

3.3. LQ controller

The step response of the water temperature of the plant by the Linear Quadratic (LQ) controller and the corresponding control action are given in Figure 3.5 and Figure 3.6, respectively.

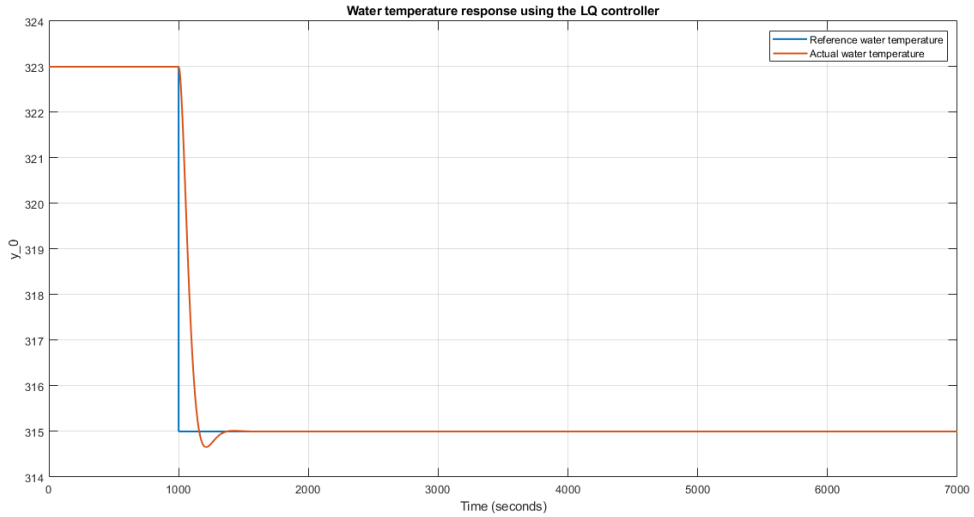

Figure 3.5: Step output for the LQ controller

As can be seen, the actual water temperature response by the LQ controller, after some settling time of 560 time instants, can reach the desired water temperature at 315°. The risetime in this particular control strategy corresponds to 106 time units, where its overshoot is 314.656.

However, the control signal shows a peak overshoot of -2.4 at the time instant of 1000 where a step change happens.

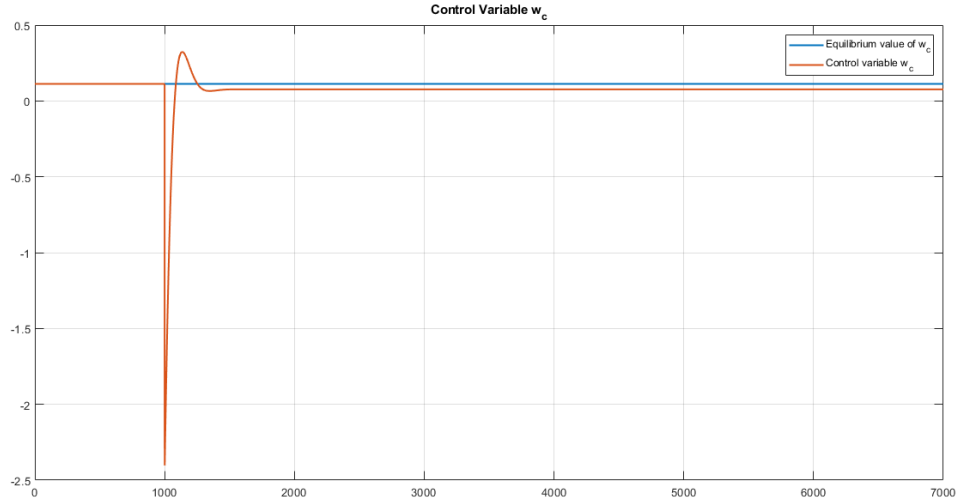

Figure 3.6: Control signal for the LQ controller

3.4. LQG controller

The step output of the water temperature in the thermo-hydraulic plant by the Linear Quadratic Gaussian (LQG) controller and its associated control action are given in the following figures:

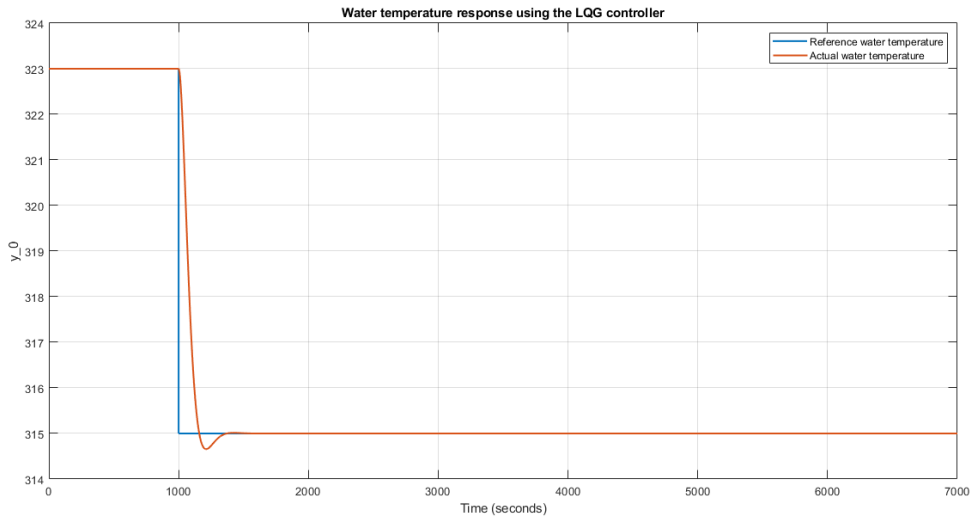

Figure 3.7: Step output for the LQG controller

As we see from Figure 3.7, the actual water temperature response by the LQG controller is able to reach the desired water temperature at 315° after some settling time of 550 time instants. The risetime in this particular control strategy corresponds to 106 time instants, where its overshoot is 314.656.

It is obvious that the main characteristics of the LQ and the LQG controllers are the same. This similarity is reflected on the control signal too, i.e., the control signal shows a peak overshoot of -2.4 at the time instant of 1000 where a step change happens.

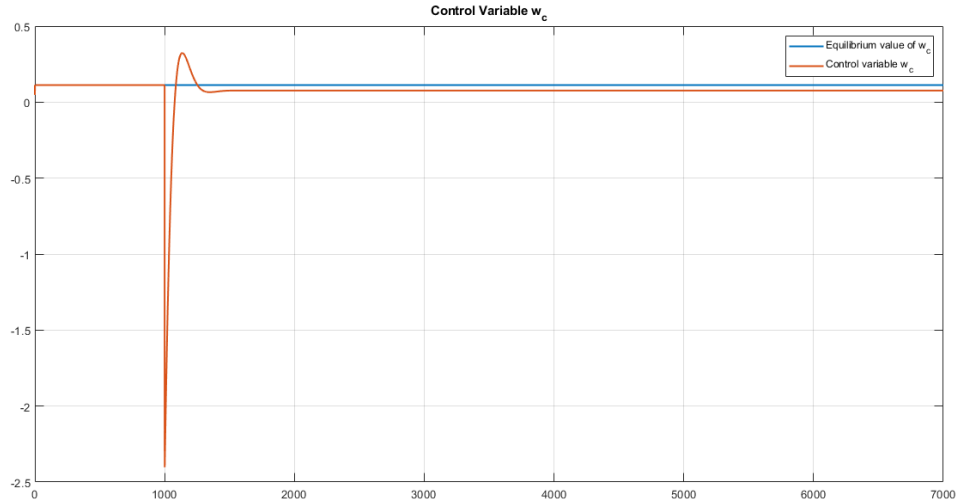

Figure 3.8: Control signal for the LQG controller

3.5. H_2 and H_∞ controllers

The step output of the water temperature in the thermo-hydraulic plant by the H_2 and H_∞ controllers and their associated control actions can be found in Figure 3.9 and Figure 3.10.

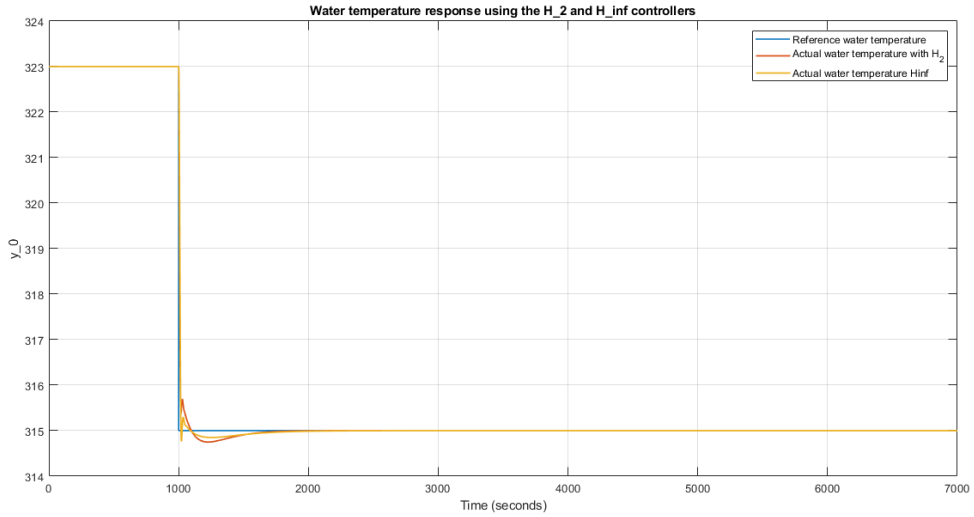

Figure 3.9: Step output for the H_2 and H_∞ controllers

As we see from Figure 3.9, the actual water temperature response by the two controllers is able to reach the desired water temperature at 315° after some settling time of 1200 (the H_2 controller) and 1800 (the H_∞ controller) time instants. The risetime values by the H_2 and H_∞ controllers are 7 and 13 time instants, respectively. Moreover, these controllers result in overshoot is 314.754 (the H_2 controller). and 314.762 (the H_∞ controller).

At the time instant of 1000 where a setpoint change takes place, these controllers cause very high values for control signals, as can be seen in Figure 3.10.

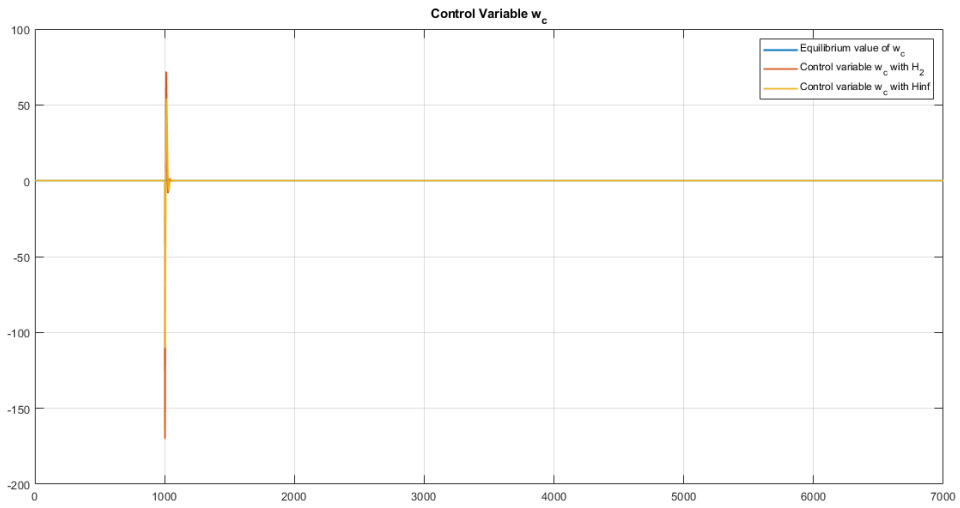

Figure 3.10: Control signal for the H_2 and H_∞ controllers

3.6. Backstepping controller

The step output of the water temperature in the thermo-hydraulic plant by the backstepping controller and its associated control action are reported in the following figures:

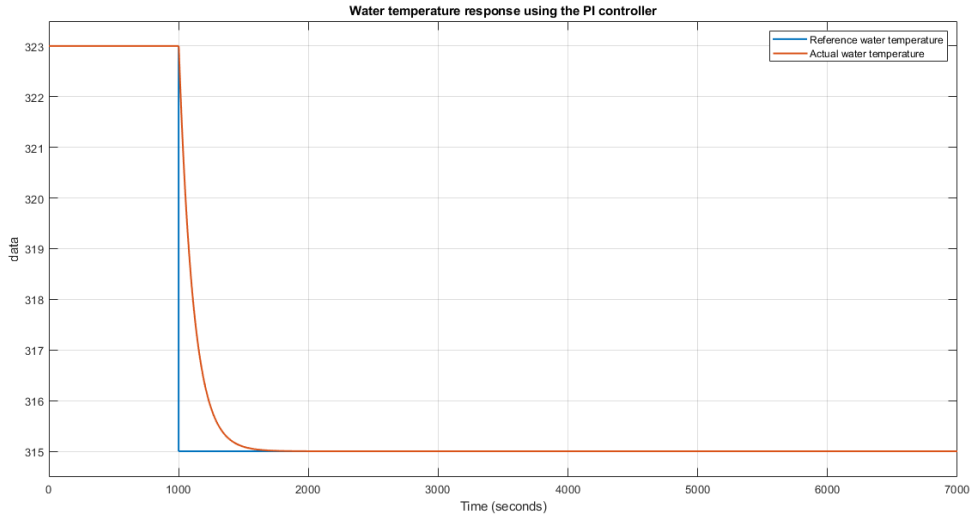

Figure 3.11: Step output for the backstepping controller

As we can see from Figure 3.11, the actual water temperature response by the backstepping controller can reach the desired water temperature at 315° after some settling time of 600 time instants. The risetime in this particular control strategy corresponds to 249 time instants, whereas there is no overshoot here.

On the other hand, control signal has an overshoot of 5.1 at the step change of the reference signal.

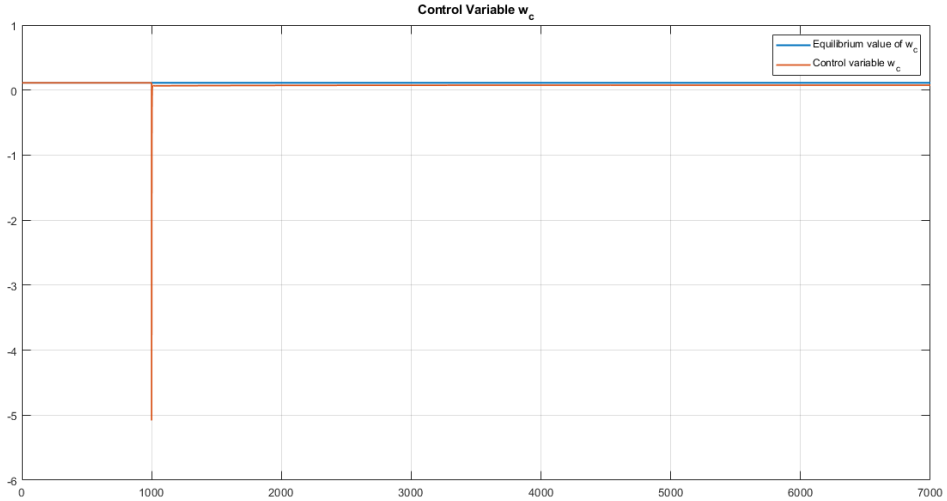

Figure 3.12: Control signal for the backstepping controller

3.7. Summary

The following table depicts the differences among the controllers designed in Chapter 2. They are compared by three parameters, namely, peak overshoot, settling time and rise time of the water temperature responses.

Controllers	Response	Step
PI	Peak overshoot	314.205
	Settling time	3200
	Rise time	476
Pole placement	Peak overshoot	-
	Settling time	450
	Rise time	112
LQ	Peak overshoot	314.656
	Settling time	560
	Rise time	106
LQG	Peak overshoot	314.656
	Settling time	550
	Rise time	106
H_2	Peak overshoot	314.754
	Settling time	1200
	Rise time	7
H_∞	Peak overshoot	314.762
	Settling time	1800
	Rise time	13
Backstepping	Peak overshoot	-
	Settling time	600
	Rise time	249

Table 3.1. Comparison in water temperature response

The table concludes that the smallest risetime of all the water temperature response by different controllers corresponds to the H_2 control, while the largest one is achieved by the PI controller. Moreover, the settling time of the PI controller shows that it is not the most preferable controller option compared to the other ones, while the LQG controller leads in the settling time category with 550 time instants.

4 Conclusion and future development

This thesis proposed the simulation and modelling of a thermo-hydraulic plant, as well as disturbance rejection caused by its load flow rate. Since the plant under study had non-linear dynamics, we implemented linearization in Chapter 1 after analyzing its mathematical model, phase plane trajectories, states, input and output variables and equilibrium points. In Chapter 2, we studied classical and optimal control problems, after which a PI controller, a pole placement controller, an LQ controller, an LQG controller, H_2 and H_∞ controllers, and a backstepping controller were designed. Finally, in Chapter 3, the performances by those controllers were compared to find out which one works best at a given condition. It turns out that the performance of the various controllers very much depends on the tuning adopted.

In general, we have synthesized those various controllers based on 7 different control strategies. For further developments, other control strategies can be developed for the thermo-hydraulic control system. Moreover, the control methods considered in this thesis can be applied on a real thermo-hydraulic plant. By doing so, we can check the performance of the plant at different operating conditions. Nonetheless, some more additional work will be needed to realize it.

Bibliography

R. Scattolini, “Lecture notes in Advanced Multivarible Control” at Politecnico di Milano, May 2020.

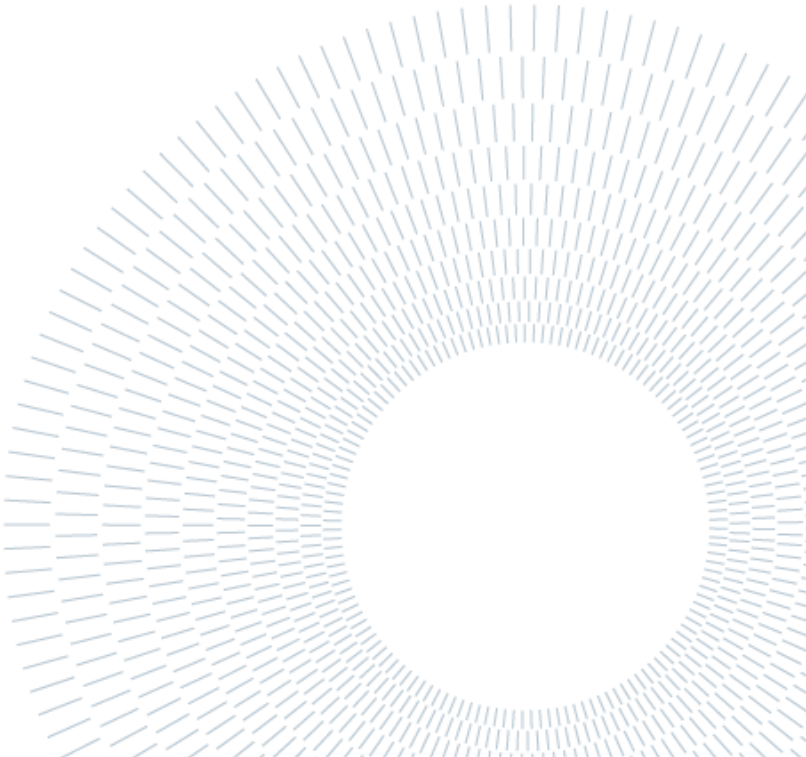

Appendix A

Here we introduce the main MATLAB script codes used in the thesis development to enrich the content of the work.

dati_sistema_termico_idraulico.m

```
close all %#ok<*NOPTS>

% PARAMETERS of the thermo-hydraulic plant
% around the central equilibrium condition (wbar=1)
zbar=2;
wbar=1;
rho=900;
A=pi/4;
c=4180;
Tbar=323;
Tibar=298;
Tmbar=363;
rhom=7860;
cm=481;
delta=0.1;
Mm=617.32;
sigma=5.67*10^(-8);
klm=3326.4;
Tf=1200;
wcbar=0.112;
kf=8;
```

PI control

```
dati_sistema_termico_idraulico
sim('openloop_response')

A3=openloop_response_Timed_Based_Linearization.a;
B3=openloop_response_Timed_Based_Linearization.b;
C3=openloop_response_Timed_Based_Linearization.c;
D3=openloop_response_Timed_Based_Linearization.d;

s = tf([1, 0],[0,1])
Gs1 = C3*((s*eye(2) - A3)^(-1))*B3+D3

%% Partition for loop wc to T
A_pi = A3
B_pi = B3(:,2)
C_pi = C3(1,:)
D_pi = 0
G = C_pi*((s*eye(2) - A_pi)^(-1))*B_pi+D_pi

%% Regulator coefficients
num = [0.018134  0.018134*0.001198];
den=[1 0];
Reg_pi =  tf(num, den)
Kp = 0.018134;
Ki = 0.018134*0.001198;

%% Loop tf
L = G * Reg_pi

%% Sensitivity
S = 1/(1+L)
```

Pole-placement for an enlarged system

```
dati_sistema_termico_idraulico
sim('openloop_response')

A3=openloop_response_Timed_Based_Linearization.a;
B3=openloop_response_Timed_Based_Linearization.b;
C3=openloop_response_Timed_Based_Linearization.c;
D3=openloop_response_Timed_Based_Linearization.d;

s = tf([1, 0],[0,1])
Gs1 = C3*((s*eye(2) - A3)^(-1))*B3+D3

A_en = A3
B_en = B3(:,2)
C_en = C3(1,:)
D_en = 0
G = C_en*((s*eye(2) - A_en)^(-1))*B_en+D_en
SysMatrix = [ -A_en, -B_en; C_en, D_en]
rank(SysMatrix)

s = tf([1, 0],[0,1]);
G_en = C_en*((s*eye(2) - A_en)^(-1)) * B_en + D_en

A_tilde = [ A_en, zeros(2, 1);
 -C_en(1, :), 0]

B_tilde = [ B_en;
 0]

M_tilde = [ 0;0;1]

Ken = place(A_tilde, B_tilde, [-0.01, -0.01001, -0.02])
Ken_x = Ken(:, 1:2)
Ken_eta = Ken(:, 3)

cl_enlarged_sys = ss(A_tilde - B_tilde * Ken, M_tilde, eye(3, 3), 0)
tf(cl_enlarged_sys)
```

LQ control for an enlarged system

```
dati_sistema_termico_idraulico
sim('openloop_response')

A3=openloop_response_Timed_Based_Linearization.a;
B3=openloop_response_Timed_Based_Linearization.b;
C3=openloop_response_Timed_Based_Linearization.c;
D3=openloop_response_Timed_Based_Linearization.d;

s = tf([1, 0],[0,1])
Gs1 = C3*((s*eye(2) - A3)^(-1))*B3+D3

A_en = A3
B_en = B3(:,2)
C_en = C3(1,:)
D_en = 0
G = C_en*((s*eye(2) - A_en)^(-1))*B_en+D_en
SysMatrix = [ -A_en, -B_en; C_en, D_en]
rank(SysMatrix)

s = tf([1, 0],[0,1]);
G_en = C_en*((s*eye(2) - A_en)^(-1)) * B_en + D_en

A_tilde = [ A_en, zeros(2, 1);
 -C_en(1, :), 0]

B_tilde = [ B_en;
 0]

M_tilde = [ 0;0;1]

% Ken = place(A_tilde, B_tilde, [-1, -1.0001, -2])
% Ken_x = Ken(:, 1:2)
% Ken_eta = Ken(:, 3)

% cl_enlarged_sys = ss(A_tilde - B_tilde * Ken, M_tilde, eye(3, 3), 0)
% tf(cl_enlarged_sys)

Q_lq = diag([1, 1, 1]);
R_lq = 0.1;

rank(ctrb(A_tilde, B_tilde))
Cq = sqrt(Q_lq)
assert(all(Cq .' * Cq - Q_lq < 1e-6, 'all'))
rank(obsv(A_tilde, Cq))

[ K_lq, P_bar, PREC] = lqr(A_tilde, B_tilde, Q_lq, R_lq)
K_lqx   = K_lq(:, 1:2);
K_lqeta = K_lq(:, 3);

L = K_lq*(s*eye(3)-A_tilde)^(-1)*B_tilde

[p,n]=size(C_en);
```

LQG control

```
dati_sistema_termico_idraulico
sim('openloop_response')

A3=openloop_response_Timed_Based_Linearization.a;
B3=openloop_response_Timed_Based_Linearization.b;
C3=openloop_response_Timed_Based_Linearization.c;
D3=openloop_response_Timed_Based_Linearization.d;

s = tf([1, 0],[0,1])
Gs1 = C3*((s*eye(2) - A3)^(-1))*B3+D3

A_en = A3
B_en = B3(:,2)
C_en = C3(1,:)
D_en = 0
G = C_en*((s*eye(2) - A_en)^(-1))*B_en+D_en
SysMatrix = [ -A_en, -B_en; C_en, D_en]
rank(SysMatrix)

s = tf([1, 0],[0,1]);
G_en = C_en*((s*eye(2) - A_en)^(-1)) * B_en + D_en
A_tilde = [ A_en, zeros(2, 1);
 -C_en(1, :), 0]
B_tilde = [ B_en;
 0]
M_tilde = [ 0;0;1]

Q_lq = diag([1, 1, 1]);
R_lq = 0.1;

rank(ctrb(A_tilde, B_tilde))
Cq = sqrt(Q_lq)
assert(all(Cq .' * Cq - Q_lq < 1e-6, 'all'))
rank(obsv(A_tilde, Cq))

[ K_lq, P_bar, PREC] = lqr(A_tilde, B_tilde, Q_lq, R_lq)
K_lqx   = K_lq(:, 1:2);
K_lqeta = K_lq(:, 3);

%% Kalman Filter
C_y = [1,  0; 0,  1];
D_y = zeros(2, 1);
Q_kf = diag([1, 1]);
R_kf = 0.1;
C_qkf = sqrt(Q_kf); % We can do this because Q_kf is diagonal!!
assert(all(C_qkf.' * C_qkf -Q_kf < 1e-6, 'all'));   % Verify that C_qkf' *
C_qkf == Q_kf with 1e-6 accuracy

reach_check = rank(ctrb(A_en, C_qkf.'))
obs_check = rank(obsv(A_en, C_y))
L_kf = lqr(A_en.', C_y.', Q_kf, R_kf).'
delta_x0_hat = zeros(2, 1);
```

H_2 and H_∞ control

```
dati_sistema_termico_idraulico
sim('openloop_response')

A3=openloop_response_Timed_Based_Linearization.a;
B3=openloop_response_Timed_Based_Linearization.b;
C3=openloop_response_Timed_Based_Linearization.c;
D3=openloop_response_Timed_Based_Linearization.d;

s = tf([1, 0],[0,1])
Gs1 = C3*((s*eye(2) - A3)^(-1))*B3+D3

A_siso = A3
B_siso = B3(:,2)
C_siso = C3(1,:)
D_siso = 0
G = C_siso*((s*eye(2) - A_siso)^(-1))*B_siso+D_siso
G = ss(G);
[n,m]=size(B_siso);
[p,n]=size(C_siso);

% definition of the shaping functions
% and Bode diagrams
wB = 10;     % desired closed-loop bandwidth
AA = 1.0000e-08;  % desired disturbance attenuation inside bandwidth
M = 2;      % desired bound on hinfnorm(S) & hinfnorm(T)
s=tf('s'); % Laplace transform variable 's'
WS=(s/M+wB)/(s+wB*AA); % Sensitivity weight
WK=(0.0001*s+1)/(0.001*s+1);  % Control weight can't be empty (d12).ne.0)
WT=(s+wB/M)/(AA*s+wB); % Complementary sensitivity weight
figure(1)
bode(WS)
hold on
bode(WK)
bode(WT)
grid
legend('WS','WK','WT')

% shaping functions written in block form

WWS=blkdiag(WS,WS,WS);
WWT=blkdiag(WT,WT,WT);
WWK=blkdiag(WK,WK,WK);

% enlarged system withshaping functions

SW = augw(G,WS,WK,WT);
[KW,CLW,GAMW,INFOW]=hinfsyn(SW);

LKW=G*KW;
SKW=inv(eye(p)+LKW);  % Sensitivity
TKW=eye(p)-SKW;       % complementary sensitivity
clear sigma
figure(2)
```

```
subplot(1, 2, 1)
sigma(T)
hold on
sigma(TKW)
title('comparison of complementary sensitivities of LGQ and H_o_o shaping
functions')
legend('T of LQG','T of Hoo')

[KW2,CLW2,GAMW2,INFOW2]=h2syn(SW);

LKW2=G*KW2;
SKW2=inv(eye(p)+LKW2);  % Sensitivity
subplot(1, 2, 2)

TKW2=eye(p)-SKW2;       % complementary sensitivity
clear sigma
sigma(T)
hold on
sigma(TKW2)
title('comparison complementary sensitivities of LGQ and H_2 shaping
functions')
legend('T of LQG','T of H_2')
sigma=5.67*10^(-8);
```

Backstepping control law

```
function y = fcn(u, w, Tref)

zbar=2;
rho=900;
A=pi/4;
c=4180;
Tbar=Tref;
Tibar=298;
Tmbar=363;
cm=481;
Mm=617.32;
sigma=5.67*10^(-8);
klm=3326.4;
Tf=1200;
kf=8;
f1 = w*Tibar/(rho*A*zbar);
f2 = w/(rho*A*zbar);
f3 = klm*A/(c*rho*A*zbar);
func1 = f1 -Tbar*f2 + f3*(Tmbar-Tbar) - u(1)*(f2+f3);
g1 = f3;
func2 = f4*(u(2)-u(1)+Tmbar-Tbar)+0.112*g2;
g2 = f6*(Tf^4-(u(2)+Tmbar)^4);
fi = (-f1+Tbar*f2-f3*(Tmbar-Tbar)-u(1))/f3;

y = 1/g2 * ((-1/f3)*(func1+f3*u(2))-0.0009*(u(2)-fi)-u(1)*g1-func2);
```